Desalination and Water Treatment
www.deswater.com
doi: 10.5004/dwt.2019.24929

172 (2019) 235–253
December

Elimination of antibiotic resistance in treated urban wastewater by iron-based advanced oxidation processes

Idil Arslan Alaton[a,*], Ayten Yazgan Karataş[b,*], Öznur Pehlivan[b], Tugba Olmez Hanci[a]

[a]*School of Civil Engineering, Department of Environmental Engineering, Istanbul Technical University, 34469 Maslak, Istanbul, Turkey, emails: arslanid@itu.edu.tr (I.A. Alaton), tolmez@itu.edu.tr (T.O. Hanci)*
[b]*School of Science and Letters, Department of Molecular Biology and Genetics, Istanbul Technical University, 34469 Maslak, Istanbul, Turkey, emails: karatasay@itu.edu.tr (A.Y. Karataş), pehlivano@itu.edu.tr (Ö. Pehlivan)*

Received 17 May 2019; Accepted 10 September 2019

ABSTRACT

Effluents from sewage treatment works are a major source of antibiotic resistance and thus create a serious risk to public health and in ecosystems. In this work, the application of alternative advanced treatment systems including iron-based heterogeneous and homogenous photochemical advanced oxidation processes (AOPs) were examined for the elimination of antibiotic resistant bacteria and their genetic materials in tertiary treated urban wastewater. Within the scope of this study, zero-valent iron (Fe^0) and goethite (α-FeOOH)-activated hydrogen peroxide (HP) oxidation as well as UV-A light-assisted photo-Fenton and photo-Fenton-like ($Fe^{2+/3+}$/HP/UV-A) treatment systems were applied to simulated tertiary urban wastewater bearing the conjugative, multi-antibiotic resistance plasmid RP4 carrier, multi-resistant *E. coli* J53 strain. Dissolved organic carbon (DOC) removals and in particular disinfection performance (removal of antibiotic resistance) were assigned as the target parameters and compared with those of conventional disinfection processes (chlorination, ozonation and UV-C radiation) by measuring inactivation of the selected multi-resistant bacteria and their genetic materials. Among the conventional disinfection methods, UV-C treatment at low doses was most effective in bacterial inactivation and reducing the gene copy numbers, followed by chlorination at high doses, whereas ozonation resulted in appreciable DOC reduction but was not very effective in reducing the gene copy numbers even at elevated doses. Fe^0, Fe^0/HP, and α-FeOOH, α-FeOOH/HP treatment systems were successful in removing DOC but exhibited very poor performance in the elimination of multi-resistant *E. coli* J53. Regarding the homogenous, photochemical iron-based AOPs, the photo-Fenton-like process was most efficient in DOC removal, whereas photo-Fenton treatment appeared to be superior in terms of bacterial inactivation. The genetic material of multi-resistant super bacteria was not efficiently removed by the application of selected homogenous photochemical, iron-based AOPs. Conclusively, although iron-based AOPs have a great potential in this application area, apparently inactivation of super bacteria and their genes by high-dose conventional disinfection remains the best option.

Keywords: Urban wastewater; Disinfection; Iron-based advanced oxidation processes; Multi-resistant *E. coli* J54 bacteria; Antibiotic resistant bacteria; Antibiotic resistance genes

1. Introduction

The unconscious use of antibiotics to cure bacterial infections has led to serious health risks as well as growing environmental problems in aquatic and terrestrial environments. The so–called "super bacteria" which are extremely resistant to most wide-spectrum, commercially important antibiotics, originate from aquaculture, animal farms,

* Corresponding authors.

Presented at the 4th International Conference on Recycling and Reuse 2018 (R&R2018), 24–26 October 2018, Istanbul, Turkey

agricultural activities as well as hospitals and household effluent [1,2]. They are drained into the sewage treatment works where they are not effectively eliminated by conventional disinfection methods, can re-enter the drinking water sources and may harm the public health and environment [3–5]. In this way, antibiotic resistant bacteria (ARB) and their genetic materials are spreading quickly in all environmental compartments which situation renders their control and elimination from water and wastewater a difficult task. Hence, their identification, control, and elimination have attracted great attention in the recent past. It has been postulated that current disinfection technologies applied at the water and wastewater treatment works including ozonation, photolysis, chlorine, chlorine dioxide, and hydrogen peroxide (HP) bleaching in the presence of sunlight, are not sufficient to eliminate antibiotic resistance [6,7]. It is important to treat antibiotic resistance as a major environmental pollution parameter by employing more advanced treatment processes to effectively eliminate multi-resistant bacteria and genes from effluents [8–10].

Recently, several studies have reported that advanced oxidation processes (AOPs) that are most basically combinations of ozone, HP, short ultraviolet (UV-C) light irradiation and metal/metal oxide catalysts could effectively eliminate ARB and antibiotic resistance genes (ARGs) from treated wastewater [11–13]. AOPs are effective chemical oxidation methods based on the intermediacy of reactive oxygen species ($HO^{\bullet}$, $HO_2^{\bullet}$, $O_2^{\bullet-}$, etc.) capable of reacting violently with recalcitrant and/or toxic inorganic and organic pollutants [14]. In particular, iron-based AOPs (Fenton and Fenton-like treatment processes) are known to be very efficient and kinetically superior in terms of target pollutants removal rates and efficiencies [15].

Aqueous ligand-to-metal charge-transfer processes in which Fe(III) is reduced and $HO^{\bullet}$ is formed are summarized below [16].

At pH = 2.8 where the molar $Fe(OH)^{2+}/Fe^{3+}$ ratio is 1.8:

$$Fe(OH)^{2+} + h\nu \rightarrow Fe^{2+} + HO^{\bullet} \quad (\text{at } 200\ \text{nm} < \lambda < 450\ \text{nm}) \quad (1)$$

The quantum yield of the photoreduction of Fe(III)-hydroxo complexes has been reported as 0.21. The thermal ("dark") Fenton reactions are given below [17]:

$$Fe^{2+} + H_2O_2 \rightarrow Fe^{3+} + HO^{\bullet} + OH^- \qquad 63\ M^{-1}s^{-1} \quad (2)$$

$$Fe^{3+} + H_2O_2 \rightarrow Fe^{2+} + HO_2^{\bullet} + H^+ \qquad 2.0\times10^{-3}M^{-1}s^{-1} \quad (3)$$

$$Fe^{2+} + \frac{HO_2^{\bullet}}{O_2^{\bullet-}} \rightarrow Fe^{3+} + H_2O_2 \qquad 1.2\times10^{6}M^{-1}s^{-1} \quad (4)$$

However, the major limitation of homogeneous, iron-based AOPs is the requirement of strictly acidic pH (=2–5) conditions. Upon addition of chelating agents (Ethylene diamine tetraacetic acid, oxalate, citrate, etc.) into the reaction solution, the solubility of iron salts can be enhanced such that working at relatively mild pH values (≥5) is possible [12,17–23] which is important for real-scale water and wastewater treatment applications. Considering this issue, the effect of introducing oxalate to the photo-Fenton-like treatment system was also examined in the present study.

Moreover, by the use of heterogeneous iron (metal oxide, zero-valent metal) catalysts the obstacle of residual Fe species in the treated effluent can partly be overcome. For instance, activation of HP with goethite (α-FeOOH) for the treatment of water pollutants has already been explored and the reaction mechanism (interaction between is goethite and HP) is briefly given below [24]:

$$\equiv Fe^{III} + H_2O_2 \rightarrow \equiv Fe^{III}H_2O_2 \quad (5)$$

$$\equiv Fe^{III}H_2O_2 \rightarrow \equiv Fe^{II} + HO_2^{\bullet} + H^+ \quad (6)$$

$$H_2O_2 + \equiv Fe^{II} \rightarrow \equiv Fe^{III} + HO^{\bullet} + OH^- \quad (7)$$

More recently, zero-valent metals including zero-valent iron (ZVI or Fe^0) have been used to activate oxidants such as HP and initiate Fenton-like oxidation reactions in the presence of air oxygen and/or HP as shown below [25]:

$$Fe^0 + O_2 + 2H^+ \rightarrow Fe^{2+} + H_2O_2 \quad (8)$$

$$Fe^0 + H_2O_2 + 2H^+ \rightarrow Fe^{2+} + 2H_2O \quad (9)$$

$$Fe^{2+} + H_2O_2 \rightarrow Fe^{3+} + HO^{\bullet} + HO^- \quad (10)$$

In the present work, for the first time, the above-mentioned heterogeneous, iron-based AOPs using FeOOH and Fe^0 catalysts as activators were also employed.

As already mentioned, Fenton (Fe^{2+}/HP) and Fenton-like (Fe^{3+}/HP) AOPs as well as their photochemical (UV-C, UV-A-enhanced) versions are well-known and established, economically attractive treatment alternatives and thus their potential to remove micropollutants including antibiotic residuals has frequently been reported [26], whereas their effect on ARB and ARGs is a relatively untouched area [27].

Until now, only a few studies have investigated the effect of different AOPs on ARB and ARGs. Moreover, to our knowledge, a comparative study examining the effect of classical (conventional) disinfection methods, homogenous UV-A-driven as well as heterogeneous iron-based AOPs based on their inactivation performance using multi-resistant *E. coli* bacteria and their genetic material has not been explored yet.

Considering these issues, in the present study synthetic urban wastewater was prepared and subjected to treatment with the heterogeneous catalytic oxidation systems involving the activation of the common oxidant HP with goethite (α-FeOOH) and zero-valent iron (Fe^0) as well as the homogenous photo-Fenton and photo-Fenton-like treatment systems, that is, HP activated with $Fe^{2+/3+}$ salts (including oxalate) and long-UV (UV-A) light radiation. The selected treatment systems were optimized in terms of critical operation parameters (oxidant concentrations, UV doses, pH, etc.) on the basis of dissolved organic carbon (DOC) removal and compared with conventional disinfection methods (chlorination, ozonation and UV-C photolysis) in terms of elimination of

antibiotic resistance, namely multi-antibiotic resistant *E. coli* J53 bacteria and their 16S ribosomal ribonucleic acid (rRNA), *aphA* and *tetA* genes.

2. Materials and methods

2.1. Materials

2.1.1. Synthetic urban wastewater

In order to have more control over the operating variables and knowledge about the exact composition of the effluent sample, domestic wastewater was simulated according to the procedure described in Imai et al. [28]. Given the presence of humic substances in effluents of wastewater treatment plants, and because they can influence different experimental aspects such as acting as inner filters and/or photosensitizers [28–31], the reaction solution was supplemented with 4 mg L^{-1} humic acid. In this way, the synthetic urban wastewater contained both readily metabolizable and recalcitrant organic matter (in the form of humic acid). This synthetic mixture effluent was called "urban wastewater", prepared daily and stored in the fridge prior to its use. In order to mimic an average organic matter concentration (based on DOC) of tertiary treated urban effluent, this "stock" solution was diluted by a factor of five with distilled water and used directly in the experiments to avoid deterioration. For each experimental run, a fresh reaction solution was prepared. The environmental characteristics of the simulated urban wastewater in its stock solution form are presented in Table 1.

Nano-scale Fe^0 particles (NANOFER 25S) were purchased from NANO IRON (Czech Republic). The organic coating of NANOFER 25S is polyacrylic acid, which is used to stabilize the nano-scale Fe^0 particles [32].

All other materials (HP, goethite, sodium sulfite, etc.) were of analytical grade and purchased from Sigma-Aldrich (MO, USA).

2.1.2. Multi-resistant E. coli

Owing to its conjugative multi-antibiotic resistance plasmid RP4, the ampicillin (Amp^R), kanamycin (Km^R) and tetracycline (Tc^R) multi-resistant *E. coli* J53 strain (DSM 3876) and its *aphA* (kanamycin resistance gene) and *tetA* (tetracycline resistance gene) genes located on the RP4 plasmid were selected as models to examine the elimination of antibiotic resistance from simulated urban wastewater. *E. coli* J53 (DSM3876) was supplied from DSMZ as in *lyophilized form*. The *aphA* and *tetA* genes encode kanamycin phosphotransferase enzyme [33] and efflux pumps [34], respectively.

2.2. Experimental procedures

2.2.1. Conventional disinfection processes

Firstly, the synthetic, tertiary treated urban wastewater was subjected to conventional disinfection with chlorine (HOCl), ozonation and UV-C photolysis at relatively high and medium (conventional) doses. In full-scale treatment for disinfection purposes, lower doses are generally used than in the present study. For example, chlorination of tertiary urban effluent is usually practiced at 1–10 mg L^{-1}. However, it has already been demonstrated that for the effective kill of viruses and spores, conventional (classical) disinfection with active chlorine is not sufficient and higher doses are required [35]. These low doses also fail the inactivation of resistant bacteria and genes [2,7,35,36].

Further, in the present study, preliminary experiments were conducted and conditions were optimized in terms of DOC removal efficiencies obtained under these treatment conditions. More specifically, the DOC parameter was considered as another major target parameter of disinfection due to the high and complex organic carbon content of (treated) urban wastewater being typical in megacities such as Istanbul. The reaction conditions that were selected for the conventional disinfection methods are summarized in Table 2.

Table 1
Environmental characteristics of the simulated urban wastewater (undiluted stock solution)

Parameter	Value
Chemical oxygen demand (COD) (mg L^{-1})	145
Biochemical oxygen demand (BOD_7) (mg L^{-1})	88
Total organic carbon (TOC) (mg L^{-1})	52
Total suspended solids (TSS) (mg L^{-1})	17
Total phosphorus (TP) (mg P L^{-1})	2.4
NH_3–N (mg N L^{-1})	4.3
Electric conductivity (EC) (μS cm^{-1})	522
Color (Pt-Co Units)	116
pH	6.8

Table 2
Experimental conditions of the conventional disinfection methods (original wastewater DOC = 8.6 mg L^{-1}; original wastewater pH = 6.8)

Disinfection type	Chlorination[a]	Ozonation	UV-C radiation
Applied dose range	0–200 mg L^{-1} (prepared from a 45,000 mg L^{-1} stock HOCl solution)	1–10 min (corresponding to 1–9 mg mg^{-1} DOC_0 at an ozone feed rate of 9 mg min^{-1})	2–30 min (at an incident photon flux of 7.6 mW cm^{-2})
Reaction volume (mL)	200	400	200
Treatment time (min)	30	2–30	1–10

[a]At the end of this experiment (chlorination) 10% w/w (0.4 M) $NaSO_3$ was added to the reaction solution at a concentration being equivalent to 10 and 100 mg L^{-1} HOCl to stop the reaction.

At the first stage, DOC removal efficiencies were followed for the above given conventional disinfection methods. In the second stage, the synthetic urban wastewater samples were contaminated with the multi-resistant *E. coli* strains and exposed to treatment with the selected conventional disinfection methods at their optimum conditions. Before and after conventional disinfection, the inactivation performance of the selected treatment systems was examined by following the number of alive, multi-resistant *E. coli* cells as well as the gene copy numbers of 16S rRNA, *aphA* and *tetA*. The same procedures were followed during the application of heterogeneous and homogenous, iron-based AOPs.

2.2.2. Heterogeneous catalytic iron-based AOPs

Synthetic urban wastewater samples were also subjected to Fe^0 and FeOOH-activated HP oxidation. Beforehand, these treatment processes were optimized in terms of the operating pH (3.5 and 5.5) and HP concentration (0–1.0 mM) in the presence of heterogeneous Fe catalyst (Fe^0 or FeOOH; recommended/selected dose: 1 g L^{-1}). Again, firstly DOC removals were followed to evaluate the processes performances and in the second part of the treatability studies, the inactivation performance of selected heterogeneous, iron-based AOPs was examined by following the number of alive, multi-resistant *E. coli* cells as well as the gene copy numbers of 16S rRNA, *aphA* and *tetA* before and after treatment application. The experimental conditions of the heterogeneous, iron-based AOPs are given in Table 3.

2.2.3. Homogenous photochemical iron-based AOPs

Simulated tertiary urban wastewater was also exposed to homogenous, photochemical AOPs; namely Fe(II) sulfate/HP/UV-A, Fe(III)nitrate/HP/UV-A and Fe(III)-oxalate/UV-A treatment systems. Throughout these experiments, again, changes in DOC values were followed and those runs resulting in highest DOC removal rates and efficiencies were selected for the next stage where inactivation of multi-resistant *E. coli* cells, as well as the gene copy numbers of 16S rRNA, *aphA* vs. *tetA* were examined in simulated urban wastewater.

Experiments with UV-C photolysis and homogenous UV-A-assisted, iron-based AOPs were conducted in an LZC-ORG model (Luzchem Research Inc., Canada) reaction chamber (dimensions: 32 cm × 33 cm × 21 cm) equipped with a magnetic stirrer and an air fan to control the temperature during the disinfection reactions. The photoreactor set-up has been described in detail elsewhere [37]. The experimental conditions of the homogenous, iron-based AOPs are shown in Table 4.

The concentrations indicated in Table 4 for HP (2 mM or 68 mg L^{-1}) and Fe (0.2 mM or 11.2 mg L^{-1}) were selected according to our previous treatability studies (with an 8–10 mg L^{-1} background DOC content), preliminary optimization experiments conducted in real and synthetic urban wastewater, national and international guidelines, dilution and precipitation effects on the reaction solutions after treatment, pH re-adjustment, and discharge into receiving water bodies including rivers, lakes, creeks [38].

Environmental characterization of the tertiary treated urban wastewater sample was carried out according to the analytical procedures given in Standard Methods [39]. The DOC concent of the tertiary treated urban wastewater samples before and during treatments was measured on a V_{PCN} analyzer (Shimadzu, Japan). Besides, pH was followed during all experiments.

2.3. Inactivation of multi-resistant bacteria and their genetic material

2.3.1. Preparation of bacterial culture, inoculation to simulated urban wastewater and sampling

Multi-resistant *E. coli* J53 was inoculated into an Luria-Bertani broth supplemented with ampicillin (100 μg mL^{-1}), kanamycin (50 μg mL^{-1}) and tetracycline (16 μg mL^{-1}) and

Table 3
Experimental conditions of the heterogeneous iron-based AOPs (common experimental conditions: original wastewater DOC = 8.6 mg L^{-1}; original wastewater pH = 6.8; T = 25°C; V = 500 mL; treatment time = 0–80 min)

Treatment system	Fe^0	Fe^0/HP[a]	FeOOH	FeOOH/HP[a]
Fe and HP	Fe^0:1 g L^{-1}	Fe^0:1 g L^{-1}	FeOOH:1 g L^{-1}	FeOOH:1 g L^{-1}
Concentrations	–	0.2–1.0 mM HP	–	0.2–1.0 mM HP
Working pH (–)	3.5, 5.5	3.5, 5.5	3.5, 5.5	3.5, 5.5

[a]Reaction was ceased with 10% w/w (0.4 M) $NaSO_3$ addition corresponding to 1.0 mM HP.

Table 4
Experimental conditions of the photochemical iron-based AOPs (common experimental conditions: T = 25°C; V = 500 mL; Time = 0–80 min; original DOC = 8.6 mg L^{-1}; original pH = 6.8)

Treatment system	Fe(II)*/HP/UV-A	Fe(III)[a]/HP/UV-A	Fe(III)-oxalate[a]/HP/UV-A	HP/UV-A (control)
Applied concentrations	0.2 mM Fe	0.2 mM Fe	0.2 mM Fe	2 mM HP
	2 mM HP	2 mM HP	2 mM HP	Only
Working pH (–)	3.5	3.5	3.5	5.5

[a]Fe(II) source was ferrous sulfate; the Fe(III) source was ferric nitrate; oxalate was added at a Fe:$C_2O_4^{2-}$ the molar ratio of 1:3.
[b]Reactions involving Fe salts were ceased with 10% w/w (0.4 M) $NaSO_3$ addition corresponding to 1.0 mM HP.

incubated at 37°C for 16 h with shaking at 200 rpm. After incubation, cells were collected with centrifugation at 13,000 rpm for 5 min. After washing 3 times with sterile phosphate buffer (pH 7.0), the cell pellet was resuspended in the simulated urban wastewater and cell density was adjusted to OD_{625nm} 0.1. The prepared bacterial suspension was stored on ice and used for the inoculation of simulated urban wastewater at 1/100 dilution ratio just before following treatment processes. Samples were collected into sterile glass bottles just before and immediately after treatment processes, stored on ice and processed within 1 h of the collection as described below.

2.3.2. Viable cell count

100 mL of samples were used to measure the viable cells by employing the standard count technique. Bacterial cells within 100 mL of samples were collected with centrifugation at 10,000 xg for 30 min. After centrifugation, the cell pellet was resuspended in 1 mL of sterile simulated urban wastewater. Thus, the cell density in each sample was 100-fold concentrated to increase the cell capture efficiency and prevent recovery errors. 10-fold dilution series were prepared up to $1:10^6$ and 100 μL from each dilution was spread on the Luria-Bertani (LB) broth supplemented with Ampicillin (100 μg/mL), Kanamycin (50 μg/mL) and Tetracyclin (16 μg/mL) (AMP/KAN/TET/LB). After incubation at 37°C for 16 h, colonies were counted and the number of viable cells before and after treatments (N_0 and N, respectively) was calculated considering dilution factors (Table S2). Log reduction (logR) values of each treatment process were also calculated and given in Table S2. The details of the procedures were given in "Supplementary Materials".

2.3.3. Total deoxyribonucleic acid isolation

Samples with volumes ranging from 100 to 350 mL were filtered via 0.22 μm micropore filters (Millipore, USA). Then, these filters were sliced into smaller pieces and loaded to tubes containing Lysing Matrix A (MP Biomedicals, CA, USA). Total deoxyribonucleic acid (DNA) isolation was performed using FastDNA Spin Kit (MP Biomedicals, CA, USA) by following manufacturer's instructions. Quality of total DNA extraction was checked by agarose gel electrophoresis and quantification of DNA was performed with spectrophotometry (NanoDrop Technologies, USA). Total DNA samples were stored at –20°C and used in a quantitative-polymerase chain reaction (Q-PCR). The details of these procedures were given in "Supplementary Materials".

2.3.4. Real-time quantitative-polymerase chain reaction using SYBR Green I Dye

Real-time Q-PCR amplification and analysis were performed using a LightCycler® 480 instrument with software 1.5 (Roche Diagnostics, Basel, Switzerland). The "Fit Point Method" was used to determine the threshold cycle (Ct).

Real-time Q-PCR was performed using LightCycler® 480 SYBR Green I Master (Roche Diagnostics, Basel, Switzerland). 15 μL of PCR mix was composed of 3 μL of PCR-grade water, 2 μL of 10X Primer Mix, and 10 μL of 2X Master Mix. PCR mix volume was multiplied by many reactions and after careful mixing, 15 μL of this mix was added to each well of LightCycler® 480 Multiwell Plates. Then, 5 μL of template DNA was added to the appropriate well. The program starts with "Pre-Incubation" at 95°C for 5 min. "Amplification" step was set to 45 cycles of 95°C for 10 s, 55°C for 20 s and 72°C for 20 s. "Melting Curve Analysis" used to monitor the specificity of the reaction was performed at 95°C for 5 s, 55°C for 1 min and the temperature was gradually increased with a ramp rate of 0.11 (°C/s) until 97°C.

2.3.4.1. Construction of standard curves for plasmid copy number determination

To construct standard curves, 16S rRNA and *aphA* and *tetA* ARGs were amplified using PCR. Colony PCR was applied to amplify the 16S rRNA gene. Plasmid DNA isolation from *E. coli* J53 was performed using the "QIAquick Plasmid DNA Isolation Kit" (QIAGEN) and the isolated plasmid DNA was used as a template for the amplification of antibiotic-resistance genes. PCR amplifications were performed using the "DreamTaq Polymerase" Kit (Thermo Fisher Scientific, MA, USA). PCR amplifications were performed using MultiGene™ OptiMax Thermal Cycler (LabNet) using following conditions: Initial denaturation at 95°C for 3 min, 35 cycle of 95°C for 30 s, 55°C for 30 s and 72°C for 1 min and final extension at 72°C for 5 min. Amplified PCR products were purified from the gel by using "NucleoSpin® Gel and PCR Clean-up Kit" (Macherey-Nagel, Düren, Germany). Purified PCR fragments were then cloned into the "pGEM®-T Easy" T/A cloning vector (Promega). The details of the process were given in "Supplementary Materials".

Standard curves were constructed as previously described by Lee et al. [40]. Standard plasmid DNA concentrations were measured with NanoDrop (USA) instrument and copy number in the stock sample was calculated by the formula given below;

$$\mathrm{DNA(copy)} = \frac{6.02 \times 10^{23}\,(\mathrm{copy/mol}) \times \mathrm{amount\ of\ DNA(g)}}{\mathrm{DNA\ length(bp)} \times 660\,(\mathrm{g/mol/bp})} \quad (11)$$

Following the calculations, 10-fold dilution series of plasmid was prepared to range from 1×10^5 to 1×10^9 copies μL^{-1}. Ct values of each dilution were determined by real-time Q-PCR using the reaction conditions and mixtures as described above. Then, standard curves were plotted by the Ct values against the logarithm of the initial template copy numbers. Finally, the gene copy numbers were calculated by using the Ct value of test samples based on the standard curves (Figs. S6, S8 and S10) and presented in Tables S3–S5.

3. Results and discussion

3.1. Conventional disinfection methods

Common oxidants such as chlorine (typically hypochlorite and hypochlorous acid) and peroxides (HP, persulfate, peracetate, etc.) are used for disinfection and known to penetrate the cells of the bacteria, thus becoming effective in removing ARB and even their genes [7]. In the present study, first, the performance of the conventional disinfection experiments was evaluated by measuring changes in the

DOC content of the samples and calculating the respective removal efficiencies. Considering the initial and final DOC values being measured during the conventional disinfection experiments, DOC removal was only observed during the ozonation of the simulated tertiary urban wastewater at a high ozone dose (for 10 min at 9 mg O_3 min^{-1}). Under these circumstances, 28% DOC removal was obtained at the end of 10 min ozonation. This is not surprising since complete oxidation (mineralization) is only expected under "harsh treatment conditions", that is, in the presence of relatively strong oxidants such as ozone being a more powerful and hence less selective oxidant than active chlorine and HP. In light of the obtained findings (DOC removal rates and efficiencies) and previous related scientific literature reports [2,7,41], it was decided to follow the fate of multi-antibiotic resistant *E. coli* bacteria under the experimental conditions given below (common experimental conditions: DOC = 8.6 mg L^{-1}; pH = 5.5–6.0; T = 25°C; V = 500 mL):

- Chlorination with 10 and 100 mg L^{-1} HOCl for 30 min
- Ozonation at a rate of 9 mg O_3 min^{-1} for 1 and 5 min
- UV-C radiation at 7.6 mW cm^{-2} for 5 and 20 min

Samples collected before and after the treatment conditions given in Table 3 were used for the viable cell count of multi-antibiotic resistant *E. coli* J53. Decadic log reductions in viable cell counts obtained after the treatment of synthetic urban wastewater spiked with resistant bacteria are displayed in Fig. 1. As can be seen in Fig. 1, 10 and 100 mg L^{-1} chlorination resulted in 5.48 ± 0.16 log reduction in viable cell numbers, whereas UV-C treatment for both 5 and 20 min resulted in a 6.01 ± 0.06 log reduction in viable cell numbers (Table S2) On the other hand, 1 and 5 min ozonation caused only 0.15 ± 0.1 and 4.78 log reductions in viable cell numbers, respectively (Table S2), from which it can be concluded that under the selected disinfection conditions, chlorination and UV-C radiation outperformed ozonation in terms of *E. coli* inactivation. Consequently, chlorination with 10 mg L^{-1} (30 min), ozonation at 9 mg min^{-1} (5 min) and UV-C treatment at 7.6 mW cm^{-2} for 5 min were determined as the most effective experimental conditions for inactivation.

Previous studies have demonstrated that inactivation of ARB is possible provided that sufficiently high disinfectant doses are applied. For example, it has been evidence that chlorine at high doses as well as reactive oxygen species produced during water and wastewater ozonation damage bacterial cell walls resulting in cell lysis [42–44]. UV-C radiation causes dimerization of bacterial DNA pyrimidine bases preventing molecular processes such as replication and transcription, ultimately leading to efficient inactivation of even of the resistant bacteria [45]. Similarly, Kim et al. [46] claimed that under longer UV-C exposure, the total DNA concentration of *E. coli* decreased, suggesting nucleic acid damage in *E. coli*. In the present study, Q-PCR was performed to determine copy numbers of ARG along with the 16S rRNA gene using total DNA extracted from the treatment samples. The logR values calculated for reductions in copy numbers of these genes obtained after chlorination, ozonation and UV-C radiation are depicted in Fig. 2.

As is evident in Fig. 2, an increase in oxidant dose/of oxidant contact time favored resistant gene damage. For chlorination, even though 10 and 100 mg L^{-1} chlorination were equally-effective on viable cell reduction, 10 mg L^{-1} chlorination (Fig. 2) reduced copy numbers of 16S rRNA, *aphA* and *tetA* less than 1-log whereas 100 mg L^{-1}-chlorination

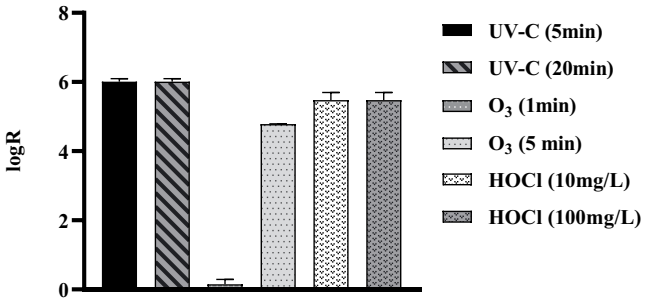

Fig. 1. LogR values obtained after conventional disinfection processes, UV-C treatment, ozonation, and chlorination. Error bars indicated standard deviations of repeated measurements. LogR indicates logarithmic reduction which represents the antimicrobial effect of treatment on resistant *E. coli* J53. LogR stands for log(N_0/N), where N_0: Initial concentration of resistant *E. coli* J53 in samples before treatment; N: Concentration of resistant *E. coli* J53 after treatment.

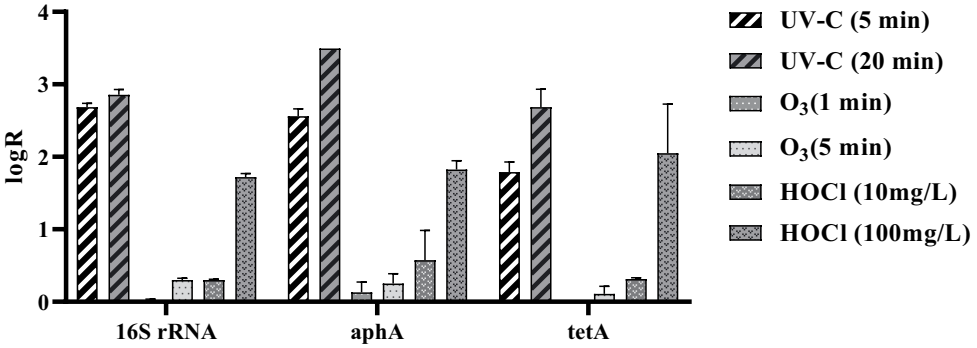

Fig. 2. LogR values of gene copy numbers obtained after conventional disinfection processes, UV-C treatment, ozonation, and chlorination. Error bars indicated standard deviations of repeated measurements. LogR indicates logarithmic reduction which represents the reduction in gene copy numbers. LogR stands for log(C_0/C), where C_0: initial gene copy numbers before treatment; C: gene copy numbers after treatment. All corresponding values (C_0, C, logR) were given in Tables S3–S5.

reduced these gene copy numbers by 1.72 ± 0.03, 1.82 ± 0.09 and 2.05 ± 0.48 log values, respectively. On the other hand, during ozonation (Fig. 2), the copy number change was less than 1 log even though viable cell reduction was high and similar to UV-C treatment (Figs. 1 and 2) The copy numbers of 16S rRNA, *aphA* and *tetA* genes during UV-C treatment reduced by approximately 3 log, until 5 min, while there was only a slight change between 5 min and 20 min UV-C treatment compared to 0–5 min ozonation. The obtained results implied that in particular for the oxidants (ozone, chlorine) high concentrations were necessary for efficient inactivation.

According to the related scientific literature [11], classical disinfection processes using ozone, chlorine and UV-C light can all induce DNA damages and thus interrupt DNA replication and/or deactivate the ARGs expression. However, their actual performances in the reduction of antibiotic resistance depend on the wastewater characteristics, as well as operation conditions, such as ozone dose, UV-C intensity and contact time with the resistant bacteria [13]. It is important to note here that the ARG concentrations in the treated effluent after ozone disinfection were a little higher than those of the other selected disinfection methods, indicating that ozonation was relatively less effective in reducing ARGs than UV-C treatment and chlorination. A few studies have also reported that ozone doses commonly used for disinfection could not significantly eliminate the antibiotic resistance in wastewater effluents [47,48] which is also in accord with our treatment results. An important reason for this evidence might be that ozone as the stronger oxidant tends to be primarily consumed by the abundant DOC (natural organic matter) present in the effluents and hence less would be available for bacterial inactivation. This is not expected for chlorination and hence might explain the findings of the present study, where appreciable inactivation could only be reached at high ozone doses (at a contact time of 5 min).

In former related work, an ozonation time of 30 min at lower doses led to log reductions ranging from 4.2 ± 0.5 to over 6.7 for the 16S rRNA and *blaTEM* genes, corresponding to 99.99% removals. Relatively low log reductions were observed after 15 min contact time, varying between 2.3 ± 0.3 and 3.7 ± 0.1 for the 16S rRNA and *intI1* genes, respectively, corresponding to 99.6% reduction, emphasizing that low doses fail efficient inactivation. After 60 min of ozonation, no quantifiable amount of DNA could be extracted from the treated synthetic wastewater [41]. UV-C radiation led to similar log reduction values of 2.1 ± 0.5 and 2.0 ± 0.3, corresponding to approximately 98.7% removal of the gene 16S rRNA [2]. These results again emphasize that oxidant concentration and/or contact time are critical for the achievement of high inactivation rates, in particular for ozonation.

In another related study, Zhuang et al. [49] compared chlorination, UV-C radiation, and ozonation for the removal of target ARGs, namely *intI1*, *tetG*, *sul1*, from a real urban wastewater sample. The most effective method was chlorination (chlorine dose of 160 mg L^{-1} and contact time of 120 min for 3.0–3.2 log reductions of ARGs), whereas relatively poor removals were achieved by UV-C radiation (a UV-C dose of 12.5 mJ cm^{-2} for 2.5–2.7 Log reductions) and with ozonation (at an ozone dose of 177.6 mg L^{-1} for 1.7–2.6 log reductions). The effect of disinfectants may also vary according to the examined genes. For example, in the same study, the *tetG* gene (from 10^5–10^6 copies mL^{-1}) was less abundant than the *tetW* gene (6.0×10^1 copies mL^{-1}) and was removed more easily than other ARGs by ozonation. However, poor reductions (2.6 log) were observed with ozone even at high ozone doses (177.6 mg L^{-1}). In spite of these unrealistically high ozone doses used in that work, ARGs were still present in the treated wastewater after ozonation, which is in agreement with our results. The higher impact of chlorine in terms of ARGs removal was linked to its ability to penetrate the cell membrane [49], but this was only possible at high chlorine doses (10–100 mg L^{-1}), as in the present study.

3.2. Disinfection with heterogeneous, iron-based AOPs

As aforementioned, the performance of the Fe^0, Fe^0/HP, FeOOH, and FeOOH/HP heterogeneous catalytic oxidation systems in terms of bacterial inactivation is an untouched area and deserves more attention. The performance of these treatment systems was firstly evaluated based on the DOC parameter at varying HP concentrations (1 g L^{-1} Fe^0; t = 80 min; pH 3.5 and 5.5). DOC removals obtained for the Fe^0/HP processes were summarized in Table 5. As evident in Table 5, no DOC removal was obtained for Fe^0 treatment in the absence of HP and Fe^0/HP treatment with 0.2 mM HP at pH 5.5 as well. However, 32% DOC removal was obtained at pH 3.5 at the same HP concentration of 0.2 mM, speaking for the requirements of lower, more acidic pH values to achieve a certain degree of oxidation. Similarly, no DOC removal was found for Fe^0/HP treatment with 0.4 mM HP at pH 5.5, whereas 54% DOC removal occurred at pH 3.5 under the same treatment conditions, again indicating that more acidic pH's were favored for effective mineralization with iron-based AOPs, as has also been postulated in former related work [14,15]. 41% DOC removal was reached after Fe^0/HP treatment at pH 3.5 with 0.6 mM HP that decreased to 35% DOC after Fe^0/HP treatment at pH 3.5 with 0.8 mM HP. 42% DOC removal was found after Fe^0/HP treatment at pH 3.5 with 1.0 mM HP. Results revealed that no further enhancement was observed upon elevating the HP concentration that speculatively might be due to the negative effect of excessive HP concentrations acting as reactive oxygen scavengers and ultimately inhibiting the oxidation of target pollutants [16,17].

HP was also activated with goethite (the FeOOH/HP treatment system) and percent DOC removals obtained under otherwise identical reaction conditions (1 g L^{-1} FeOOH; pH 3.5 and 5.5; t = 80 min) are shown in Table 6. 24% DOC removal was observed for FeOOH treatment without HP addition at pH 5.5 and 29% DOC removal for FeOOH/HP treatment with 0.2 mM HP at pH 5.5. DOC removals increased to 31% and 49% after FeOOH/HP treatments at pH 5.5 and pH 3.5, respectively, in the presence of 0.4 mM HP. As in the case of Fe^0-activated HP, the oxidation reaction was HP concentration- and especially pH-dependent. An abrupt decrease was evident beyond a critical, "optimum" HP concentration. Only 9% DOC removal was achieved for FeOOH/HP treatment at pH 3.5 in the presence of 0.6 mM HP and no DOC removal was obtained for FeOOH/HP treatment at pH 3.5 in the presence of 0.8 mM HP. A further increase to the highest studied HP concentration (1.0 mM) resulted in a poor

DOC removal of only 17% after FeOOH/HP treatment at pH 3.5 speaking for an overdose resulting in a serious inhibition of the oxidation reaction. As in the case of activation with Fe^0, the oxidation system involving FeOOH required careful optimization of pH and oxidant concentration for effective oxidation (mineralization).

Considering the above findings shown for the Fe^0/HP and FeOOH/HP heterogeneous catalytic oxidation processes, it was decided to further inspect the fate of resistant *E. coli* bacteria under the following experimental conditions:

- Fe^0/HP treatment process: 1 g L^{-1} Fe^0; 0.4 mM HP; 20 min; pH = 3.5
- FeOOH/HP treatment process: 1 g L^{-1} FeOOH; 0.4 mM HP; 60 min; pH = 3.5

Samples collected before and after treatment under the selected Fe^0/HP and FeOOH/HP reaction conditions were used for the viable cell count of multi-antibiotic resistant *E. coli* J53. According to the experimental results, both Fe^0 and FeOOH-activated HP treatments resulted in very poor inactivation (the log reduction in viable cell numbers was below 0.2 for Fe^0/HP and less than 0.002 for FeOOH/HP), thus further Q-PCR analyses were not performed. From these results is clear that heterogeneous iron-based AOPs performed well in DOC removal (mineralization), but were not capable of bacterial inactivation. The reason has to be further explored and hence requires further investigation in the future.

3.3. Disinfection with homogenous photochemical iron-based AOPs

Synthetic urban wastewater samples were also subjected to homogenous photochemical treatment with iron-based AOPs. Fig. 3 displays changes in normalized DOC values obtained after HP bleaching with near UV-A (HP/UV-A; serving as the control experiment of this set of experiment), Fe(II)/HP/UV-A, Fe(III)/HP/UV-A and Fe(III)-oxalate/UV-A treatments of synthetic tertiary treated urban wastewater.

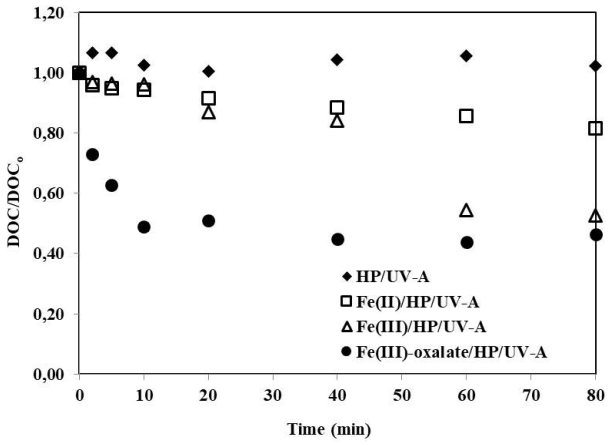

Fig. 3. Changes in normalized DOC values obtained during HP/UV-A, Fe(II)/HP/UV-A, Fe(III)/HP/UV-A and Fe(III)-oxalate/UV-A treatments of simulated tertiary urban wastewater. Experimental conditions: original DOC = 8.6 mg L^{-1}; original pH = 6.8; Fe = 0.2 mM; $C_2O_4^{2-}$ = 0.6 mM for the Fe(III)-oxalate/UV-A process (to achieve a Fe:oxalate molar ratio of 1:3); HP = 2 mM; UV-A radiation intensity = 5.4 mW cm^{-2}; t = 80 min; V = 500 mL; T = 25°C.

As is obvious from Fig. 3, no DOC removal was obtained for the control experiment (HP/UV-A), which is not surprising. DOC fluctuated during HP/UV-A treatment and the lowest DOC value (7.92 mg L^{-1}) was measured at t = 20 min. Hence, a treatment time of 20 min was selected to be appropriate for HP/UV-A treatment to be used in the forthcoming set. Mineralization was observed in the presence of Fe(II); Fe(II)/HP/UV-A and Fe(III)/HP/UV-A treatments resulted in 18% and 39% DOC removals after 80 min treatment, respectively.

In the presence of oxalate ions, the overall, relative DOC removal rate increased to 54% after 80 min treatment with the Fe(III)-oxalate/UV-A process. However, since organic carbon was externally added as oxalate to the reaction solution, although the highest DOC removal efficiency was achieved for this photochemical treatment process, there was still a DOC of 8.2 mg L^{-1} in the treated effluent, which was as high as the original DOC in the reaction solution. Considering the above treatment results, it was decided to select the following homogenous photochemical iron-based AOPs for further inactivation assessment:

- t = 80 min for Fe(II)-(III)/HP/UV-A and t = 20 min for HP/UV-A (control experiment);

Hence, Fe(III)/oxalate/UV-A was not further examined due to the high, final DOC content of the reaction solution after photochemical treatment.

Fig. 4 presents logR reductions in resistant *E. coli* after the application of homogenous photochemical iron-based AOPs under the selected reaction conditions (treatment time). From Fig. 4 it can be seen that the highest logR reduction was obtained for Fe(II)/HP/UV-A treatment with 4.82 ± 0.04, followed by Fe(III)/HP/UV-A and HP/UV-A, whose inactivation (logR values) rates were close to each other, namely 3.85 ± 0.01 and 3.44 ± 0.05, respectively. Although the mineralization rate of the photo-Fenton-like reaction was higher than for photo-Fenton treatment, photocatalysis involving a ferrous iron salt resulted in superior inactivation rates that might be linked to the importance of direct involvement of the thermal Fenton (Haber–Weiss) chain reactions in bacterial inactivation [50,51].

From the results shown in Fig. 4, it is particularly obvious that the logR value being achieved for HP/UV-A treatment is comparable with that observed for the photo-Fenton-like processes in terms of resistant genes. Similarly, Acra et al. [52] have reported that UV-A and short visible wavelengths (320–450 nm) were able to generate reactive oxygen species in the presence of HP which may cause strand breakage and changes in DNA. These toxic reactive oxygen species can also disrupt protein synthesis. Moreover, UV-B (290–320 nm) is known to directly induce DNA damage via the formation of the inhibitory cyclobutane pyrimidine dimer photoproduct [53]. The formation of these dimers causes genetic mutation, inhibits DNA replication and alters gene expression [53].

LogR values of gene copy numbers obtained after the treatment of synthetic urban wastewater with homogenous,

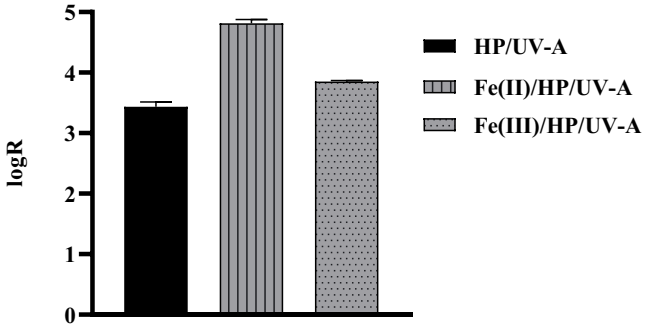

Fig. 4. LogR values for resistant *E. coli* J53 counts after treatment of synthetic urban wastewater with homogenous, photochemical iron-based AOPs and HP/UV-A. Error bars indicated standard deviations of repeated measurements. LogR indicates logarithmic reduction which represents the antimicrobial effect of treatment on resistant *E. coli* J53. LogR stands for $\log(N_0/N)$, where N_0: initial concentration of resistant *E. coli* J53 in samples before treatment; N: concentration of resistant *E. coli* J53 after treatment. Experimental conditions are as in Fig. 3.

photochemical, iron-based AOPs were also determined. The selected treatment methods were not effective in the reduction in genetic material with logR reductions below 0.5 (Tables S3–S5).

It has also been elucidated that HP/sunlight treatment and in particular the photo-Fenton processes bring about oxidation by the generation of highly reactive oxygen species that can be used for cell inactivation. These species are capable of killing bacteria mainly by destroying their cell membranes or walls [33]. Bianchini et al. [43] claimed the formation of $HO^{\bullet}$ and carbon-centred radicals during treatment of wastewater with Fenton-like processes, whereas Kikuchi et al. [44] suggested that possibly superoxide radicals ($O_2^{\bullet -}$) and HP can diffuse into microorganisms' cell through the membrane and produce $HO^{\bullet}$ by the Haber–Weiss reaction [12]:

$$O_2^{\bullet -} + HP \rightarrow O_2 + HO^{\bullet} + HO^{-} \quad (12)$$

4. Conclusions and recommendations

In the present study, the application of heterogeneous and homogenous iron-based AOPs to inactivate resistant bacteria and their genetic material was investigated in simulated tertiary treated urban wastewater.

The following conclusions could be drawn from the present study;

- Considering the DOC parameter that was followed during the conventional disinfection experiments as the target parameter, an appreciable DOC removal (28%) could only be achieved after high-rate ozonation (9 mg min^{-1} and 5–10 min) of the simulated urban effluent.
- Both 10 and 100 mg L^{-1} chlorination resulted in a 5.48 ± 0.16 log reduction in viable cell numbers. 1 min ozonation at 9 mg min^{-1} caused approximately 0.15 ± 0.1 log reduction and 5 min ozonation resulted in 4.78 log reduction in viable cell counts. UV-C treatment for 5 and 20 min resulted in 6.01 ± 0.06 log reduction in viable cell numbers.
- Conclusively, UV-C treatment for 5 min, ozonation for 5 min and chlorination at 10 mg L^{-1} for 30 min were determined as the most effective experimental disinfection conditions in terms of bacterial inactivation.
- Even though 10 and 100 mg L^{-1} chlorination were equally effective in viable cell reduction; 10 mg L^{-1} chlorination reduced the copy numbers of 16S rRNA, *aphA* and *tetA* by less than 1 log, while 100 mg L^{-1}-chlorination reduced the copy numbers of the genes by 1.72 ± 0.03, 1.82 ± 0.09 and 2.05 ± 0.48, respectively, emphasizing the requirement of high chlorine doses for removal of genetic material. For high-rate ozonation, the change in copy numbers was less than 1 log even though viable cell reduction was obtained similar to UV-C treatment. The copy numbers of 16S rDNA, *aphA* and *tetA* genes during UV-C treatment were reduced by approximately 3 log until 5 min. There was only a slight change between 5 and 20 min UV-C treatment compared with UV-C radiation in the 0–5 min dose range.
- UV-C treatment at 7.6 mW cm^{-2} for 5 min appeared to be the most effective method in reducing the gene copy numbers, followed by chlorination at 100 mg L^{-1} (high dose disinfection), whereas ozonation at 9 mg min^{-1} (high dose ozonation) was not very effective in reducing the gene copy numbers, even at the highest tried dose (10 min at 9 mg min^{-1}).
- Both pH and HP concentration played a critical role in DOC removal with the heterogeneous, iron-based AOPs

Table 5
DOC removal efficiencies observed for the Fe^0/HP treatment system (common experimental conditions: original DOC = 8.6 mg L^{-1}; pH = 3.5 and 5.5, t = 80 min)

Treatment system	DOC removal pH 3.5 (%)	DOC removal pH 5.5 (%)
Fe^0	–	0
Fe^0/0.2 mM HP	32	0
Fe^0/0.4 mM HP	54	0
Fe^0/0.6 mM HP	41	–
Fe^0/0.8 mM HP	35	–
Fe^0/1.0 mM HP	42	–

Table 6
DOC removal efficiencies observed for the FeOOH/HP treatment system (common experimental conditions: original DOC = 8.6 mg L^{-1}; pH = 3.5 and 5.5, t = 80 min)

Treatment system	DOC removal pH 3.5 (%)	DOC removal pH 5.5 (%)
FeOOH only	–	24
FeOOH/0.2 mM HP	–	29
FeOOH/0.4 mM HP	49	32
FeOOH/0.6 mM HP	17	0
FeOOH/0.8 mM HP	0	–
FeOOH/1.0 mM HP	0	–

(the Fe^0/HP and FeOOH/HP treatment systems). Fe^0 only and Fe^0/HP, as well as FeOOH only and FeOOH/HP treatments, resulted in less than 1-fold reduction in viable cell numbers. Hence, no further Q-PCR analysis was performed. Overall, the heterogeneous, catalytic iron-based AOPs were effective in DOC removal, but not in the elimination of multi-resistant *E. coli* J53.

- HP/UV-A treatment (UV-A = 5.4 mW cm^{-2}; HP = 2.0 mM; pH = 6.8; t = 20 min) was not effective in terms of mineralization, but showed almost equal performance in bacterial and genetic material inactivation compared with photochemical, iron-based AOPs. The homogenous, photochemical, iron-based AOPs (UV-A = 5.4 mW cm^{-2}; HP = 2.0 mM; $Fe^{2+/3+}$ = 0.2 mM; pH = 3.5; t = 80 min) were effective in DOC removal and inactivation of multi-resistant bacteria (logR values in the range of 3–5); but less efficient in the reduction of gene copy numbers (logR value range = 0.3–0.5) compared to classical, high-rate disinfection methods.

Both UV-A-assisted homogenous as well as heterogeneous, catalytic iron-based AOPs could not outperform conventional disinfection methods when applied at high doses in terms of bacterial inactivation and removal of genetic material. However, a generalization should be taken with caution since conditions may change and do not exclude the possibility of failure. Overall, it is a matter of economic feasibility, ecotoxicological safety, sustainability and legislative requirements [54] whether alternative, "green" disinfection methods can eventually replace the classical ones applied at high doses in the future. Working with real urban wastewater under realistic treatment conditions is highly recommended to confirm the present experimental findings. Further, real-scale treatability studies should continue to demonstrate that antibiotic resistance is a serious risk in treated urban effluent and should be regarded as a priority pollution parameter.

Acknowledgments

The authors are thankful to the financial support of Istanbul Technical University under Project Number 41117.

References

[1] J. Ory, G. Bricheux, A. Togola, J.L. Bonnet, F. Donnadieu-Bernard, L. Nakusi, C. Forestier, O. Traore, Ciprofloxacin residue and antibiotic-resistant biofilm bacteria in hospital effluent, Environ. Pollut., 214 (2016) 635–645.

[2] W. Ben, J. Wang, R. Cao, M. Yang, Y. Zhang, Z. Qiang, Distribution of antibiotic resistance in the effluents of ten municipal wastewater treatment plants in China and the effect of treatment processes, Chemosphere, 172 (2017) 392–398.

[3] G. Ferro, F. Guarino, S. Castiglione, L. Rizzo, Antibiotic resistance spread potential in urban wastewater effluents disinfected by UV/H_2O_2 process, Sci. Total Environ., 560–561 (2016) 29–35.

[4] C. Zanotto, M. Bissa, E. Illiano, V. Mezzanotte, F. Marazzi, A. Turolla, M. Antonelli, C. De Giuli Morghen, A. Radaelli, Identification of antibiotic-resistant *Escherichia coli* isolated from a municipal wastewater treatment plant, Chemosphere, 164 (2016) 627–653.

[5] J. Xu, Y. Xu, H.M. Wang, C.S. Guo, H.Y. Qiu, Y. He, Y. Zhang, X.C. Li, W. Meng, Occurrence of antibiotics and antibiotic resistance genes in a sewage treatment plant and its effluent-receiving river, Chemosphere, 119 (2015) 1379–1385.

[6] J. Ndounla, S. Kenfack, J. Wéthé, C. Pulgarín, Relevant impact of irradiance (vs. dose) and evolution of pH and mineral nitrogen compounds during natural water disinfection by photo-Fenton in a solar CPC reactor, Appl. Catal., B, 148–149 (2014) 144–153.

[7] J. Oh, D.E. Salcedo, C.A. Medriano, S. Kim, Comparison of different disinfection processes in the effective removal of antibiotic-resistant bacteria and genes, J. Environ. Sci., 26 (2014) 1238–1242.

[8] M.-T. Guo, G.-S. Zhang, Graphene oxide in the water environment could affect tetracycline-antibiotic resistance, Chemosphere, 183 (2017) 197–203.

[9] X.Y. Li, Y. Huang, C. Li, J.M. Shen, Y. Deng, Degradation of *p*CNB by Fenton like process using α-FeOOH, Chem. Eng. J., 260 (2015) 28–36.

[10] K.D. Lin, J.F. Ding, H.Y. Wang, X.W. Huang, J. Gan, Goethite-mediated transformation of bisphenol A, Chemosphere, 89 (2012) 789–795.

[11] M.T. Guo, Q.B. Yuan, J. Yang, Distinguishing effects of ultraviolet exposure and chlorination on the horizontal transfer of antibiotic resistance genes in municipal wastewater, Environ. Sci. Technol., 49 (2015) 5771–5778.

[12] A. Fiorentino, G. Ferro, M.C. Alferez, M.I. Polo-López, P. Fernández-Ibañez, L. Rizzo, Inactivation and regrowth of multidrug resistant bacteria in urban wastewater after disinfection by solar-driven and chlorination processes, J. Photochem. Photobiol., B, 148 (2015) 43–50.

[13] L. Rizzo, C. Manaia, C. Merlin, T. Schwartz, C. Dagot, M.C. Ploy, I. Michael, D. Fatta-Kassinos, Urban wastewater treatment plants as hotspots for antibiotic resistant bacteria and genes spread into the environment: a review, Sci. Total Environ., 447 (2013) 345–360.

[14] A. Safarzadeh-Amiri, J.R. Bolton, S.R. Cater, The use of iron in advanced oxidation processes, J. Adv. Oxid. Technol., 1 (1996) 18–26.

[15] A. Safarzadeh-Amiri, J.R. Bolton, S.R. Cater, Ferrioxalate-mediated solar degradation of organic contaminants in water, Sol. Energy, 56 (1996) 439–443.

[16] B.C. Faust, J. Hoigné, Photolysis of Fe (III)-hydroxy complexes as sources of OH radicals in clouds, fog and rain, Atmos. Environ. Part A, 24 (1990) 79–89.

[17] V.A. Nadtochenko, J. Kiwi, Photolysis of $FeOH^{2+}$ and $FeCl^{2+}$ in aqueous solution. Photodissociation kinetics and quantum yields, Inorg. Chem., 37 (1998) 5233–5238.

[18] N. de la Cruz, L. Esquius, D. Grandjean, A. Magnet, A. Tungler, L.F. de Alencastro, C. Pulgarín, Degradation of emergent contaminants by UV, UV/H_2O_2 and neutral photo-Fenton at pilot scale in a domestic wastewater treatment plant, Water Res., 47 (2013) 5836–5845.

[19] A. de Luca, R.F. Dantas, S. Esplugas, Assessment of iron chelates efficiency for photo-Fenton at neutral pH, Water Res., 61 (2014) 232–242.

[20] S. Papoutsakis, S. Miralles-Cuevas, I. Oller, J.L. Garcia Sanchez, C. Pulgarin, S. Malato, Microcontaminant degradation in municipal wastewater treatment plant secondary effluent by EDDS assisted photo-Fenton at near-neutral pH: an experimental design approach, Catal. Today, 252 (2015) 61–69.

[21] S. Giannakis, C. Ruales-Lonfat, S. Rtimi, S. Thabet, P. Cotton, C. Pulgarín, Castles fall from inside: evidence for dominant internal photo-catalytic mechanisms during treatment of *Saccharomyces cerevisiae* by photo-Fenton at near-neutral pH, Appl. Catal., B, 185 (2016) 150–162.

[22] A. Fiorentino, R. Cucciniello, A. Di Cesare, D. Fontaneto, P. Prete, L. Rizzo, G. Corno, A. Proto, Disinfection of urban wastewater by a new photo-Fenton like process using Cu-iminodisuccinic acid complex as catalyst at neutral pH, Water Res., 146 (2018) 206–215.

[23] A. Fiorentino, B. Esteban, J.A. Garrido-Cardenas, K. Kowalska, L. Rizzo, A. Aguera, J.A. Sánchez Pérez, Effect of solar photo-Fenton process in raceway pond reactors at neutral pH on antibiotic resistance determinants in secondary treated urban wastewater, J. Hazard. Mater., 378 (2019) 120737.

[24] W.P. Kwan, B.M. Voelker, Rates of hydroxyl radical generation and organic compound oxidation in mineral-catalyzed Fenton-like systems, Environ. Sci. Technol., 37 (2003) 1150–1158.
[25] C.R. Keenan, D.L. Sedlak, Ligand-enhanced reactive oxidant generation by nanoparticulate zero-valent iron and oxygen, Environ. Sci. Technol., 42 (2008) 6936–6941.
[26] X.C. Liu, Y.Y. Zhou, J.C. Zhang, L. Luo, Y. Yang, H.L. Huang, H. Peng, L. Tang, Y. Mu, Insight into electro-Fenton and photo-Fenton for the degradation of antibiotics: mechanism study and research gaps, Chem. Eng. J., 347 (2018) 379–397.
[27] S. Giannakis, T.-T. Melvin Le, J.M. Entenza, C. Pulgarin, Solar photo-Fenton disinfection of 11 antibiotic-resistant bacteria (ARB) and elimination of representative AR genes. Evidence that antibiotic resistance does not imply resistance to oxidative treatment, Water Res., 143 (2018) 334–345.
[28] A. Imai, T. Fukushima, K. Matsushige, Y.-H. Kim, K.S. Choi, Characterization of dissolved organic matter in effluents from wastewater treatment plants, Water Res., 36 (2002) 859–870.
[29] R. Andreozzi, M. Raffaele, P. Nicklas, Pharmaceuticals in STP effluents and their solar photodegradation in aquatic environment, Chemosphere, 50 (2003)1319–1330.
[30] A. Rodrigues, A. Brito, P. Janknecht, M.F. Proença¸ R. Nogueira, Quantification of humic acids in surface water: effects of divalent cations, pH, and filtration, J. Environ. Monit., 11 (2009) 377–382.
[31] E.M.-L. Janssen, P.R. Erickson, K. McNeill, Dual roles of dissolved organic matter as sensitizer and quencher in the photooxidation of tryptophan, Environ. Sci. Technol., 48 (2014) 4916–4924.
[32] S. Klimkova, M. Cernik, L. Lacinova, J. Filip, D. Jancik, R. Zboril, Zero-valent iron nanoparticles in treatment of acid mine water from *in situ* uranium leaching, Chemosphere, 82 (2011) 1178–1184.
[33] F.C. Tenover, P.M. Elvrum, Detection of two different kanamycin resistance genes in naturally occurring isolates of *Campylobacter jejuni* and *Campylobacter coli*, Antimicrob. Agents Chemother., 32 (1988) 1170–1173.
[34] I. Chopra, M. Roberts, Tetracycline antibiotics: mode of action, applications, molecular biology, and epidemiology of bacterial resistance, Microbiol. Mol. Biol. Rev., 65 (2001) 232–260.
[35] I. Michael-Kordatou, P. Karaolia, D. Fatta-Kassinos, The role of operating parameters and oxidative damage mechanisms of advanced chemical oxidation processes in the combat against antibiotic-resistant bacteria and resistance genes present in urban wastewater, Water Res., 129 (2018) 208–230.
[36] M.B. Ahmed, J.L. Zhou, H.H. Ngo, W. Guo, N.S. Thomaidis, J. Xu, Progress in the biological and chemical treatment technologies for emerging contaminant removal from wastewater: a critical review, J. Hazard. Mater., 323 (2017) 274–298.
[37] M. Molkenthin, T. Olmez-Hanci, M.R. Jekel, I. Arslan-Alaton, Photo-Fenton-like treatment of BPA: effect of UV light source and water matrix on toxicity and transformation products, Water Res., 47 (2013) 5052–5064.
[38] WHO, Iron in Drinking-water, Background Document for Development of WHO Guidelines for Drinking Water Quality, In: Guidelines For Drinking-Water Quality, 2nd ed., Vol. 2, Health Criteria and Other Supporting Information, World Health Organization, Geneva, 1996.
[39] APHA, Standard Methods for the Examination of Water and Wastewater, 21st ed., American Public Health Association/ American Water Works Association/Water Environment Federation, Washington D.C., USA, 2005.
[40] C. Lee, J. Kim, S.G. Shin, S. Hwang, Absolute and relative Q-PCR quantification of plasmid copy number in *Escherichia coli*, J. Biotechnol., 123 (2006) 273–280.
[41] J.M. Sousa, G. Macedo, M. Pedrosa, C. Becerra-Castro, S. Castro-Silva, M.F.R. Pereira, A.M.T. Silva, O.C. Nunes, C.M. Manaia, Ozonation and $UV_{254\,nm}$ radiation for the removal of microorganisms and antibiotic resistance genes from urban wastewater, J. Hazard. Mater., 323 (2017) 434–441.
[42] R.J. Watts, S.H. Kong, M.P. Orr, C.G. Miller, B.E. Henry, Photocatalytic inactivation of coliform bacteria and viruses in secondary wastewater effluent, Water Res., 29 (1995) 95–100.
[43] R. Bianchini, L. Calucci, C. Lubello, C. Pinzino, Intermediate free radicals in the oxidation of wastewaters, Res. Chem. Intermed., 28 (2002) 247–256.
[44] Y. Kikuchi, K. Sunada, T. Iyoda, K. Hashimoto, A. Fujishima, Photocatalytic bactericidal effect of TiO_2 thin films: dynamic view of the active oxygen species responsible for the effect, J. Photochem. Photobiol., A, 160 (1997) 51–56.
[45] P. Rusin, S. Maxwell, C. Gerba, Comparative surface-to-hand and fingertip-to-mouth transfer efficiency of gram-positive bacteria, gram-negative bacteria, and phage, J. Appl. Microbiol., 93 (2002) 585–592.
[46] S. Kim, K. Ghafoor, J.Y. Lee, M. Feng, J.Y. Hong, D.-U. Lee, J.Y. Park, Bacterial inactivation in water, DNA strand breaking, and membrane damage induced by ultraviolet-assisted titanium dioxide photocatalysis, Water Res., 47 (2013) 4403–4411.
[47] N. Czekalski, R. Sigdel, J. Birtel, B. Matthews, H. Bürgmann, Does human activity impact the natural antibiotic resistance background? Abundance of antibiotic resistance genes in 21 Swiss lakes, Environ. Int., 81 (2015) 45–55.
[48] G. Pak, D.E. Salcedo, H. Lee, J. Oh, S.K. Maeng, K.G. Song, S.W. Hong, H.C. Kim, K. Chandran, S. Kim, Comparison of antibiotic resistance removal efficiencies using ozone disinfection under different pH and suspended solids and humic substance concentrations, Environ. Sci. Technol., 50 (2016) 7590–7600.
[49] Y. Zhuang, H.Q. Ren, J.J. Geng, Y.Y. Zhang, Y. Zhang, L. Ding, K. Xu, Inactivation of antibiotic resistance genes in municipal wastewater by chlorination, ultraviolet, and ozonation disinfection, Environ. Sci. Pollut. Res., 22 (2015) 7037–7044.
[50] M.B. Fisher, K.L. Nelson, Inactivation of *Escherichia coli* by polychromatic simulated sunlight: evidence for and implications of a Fenton mechanism involving iron, hydrogen peroxide, and superoxide, Appl. Environ. Microbiol., 80 (2014) 935–942.
[51] J. Rodríguez-Chueca, A. Mediano, M.P. Ormad, R. Mosteo, J.L. Ovelleiro, Disinfection of wastewater effluents with the Fenton-like process induced by electromagnetic fields, Water Res., 60 (2014) 250–258.
[52] A. Acra, M. Jurdi, A.M.U. Allem, Y. Karahagopian, Z. Raffoul, Sunlight as disinfectant, Lancet, 333 (1989) 280.
[53] M.M. Lyons, P. Aas, J.D. Pakulski, L. Van Waasbergen, R.V. Miller, D.L. Mitchell, W.H. Jeffrey, DNA damage induced by ultraviolet radiation in coral-reef microbial communities, Mar. Biol., 130 (1998) 537–543.
[54] L. Rizzo, S. Malato, D. Antakyali, V.G. Beretsou, M.B. Dolic, W. Gernjak, E. Heath, I. Ivancev-Tumbas, P. Karaolia, A.R. Lado Ribeiro, G. Mascolo, C.S. McArdell, H. Schaar, A.M.T. Silva, D. Fatta-Kassinos, Consolidated vs new advanced treatment methods for the removal of contaminants of emerging concern from urban wastewater, Sci. Total Environ., 655 (2019) 986–1008.

Supplementary information

S1. RP4 plasmid isolation from Escherichia coli DSM 3876

A single colony was transferred into 4 mL of LB-Amp-Kan-Tet broth and incubated at 37°C overnight for plasmid isolation. Plasmid isolation was performed using the modified procedure of the "QIAquick Plasmid deoxyribonucleic acid (DNA) Isolation Kit" (QIAGEN). The isolated plasmid was run on 1% (w/v) agarose gel at 120 V for 40 min. RedSafe™ Nucleic Acid Staining Solution (iNtRON) was used to visualize gels under UV transillumination. 56 kb-plasmid products were obtained (Fig. S1)

S2. Polymerase chain reaction amplification of aphA, tetA and 16S ribosomal ribonucleic acid genes and cloning into pGEM®-T Easy Vector

Polymerase chain reaction (PCR) amplifications were performed using DreamTaq Polymerase (Thermo Fisher Scientific, MA, USA) and used primers given in Table S1. To amplify *aphA* and *tetA*, purified RP4 plasmid was used as a template. To amplify 16S ribosomal ribonucleic acid (rRNA), colony PCR was performed; therefore, a swipe of a colony was taken with a toothpick and added into the PCR reaction mixture. Amplified PCR products were run on 2.5% (w/v) agarose gel prepared with 1X TAE Buffer at 70 V for 1 h. RedSafe™ Nucleic Acid Staining Solution (iNtRON) was used to visualize gels under UV transillumination. Amplified PCR products are shown in Fig. S2.

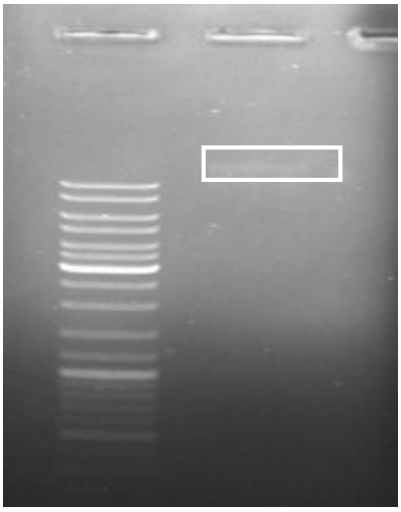

Fig. S1. Plasmid RP4 isolated from *E.coli* DSM 3876. Marker DNA: GeneRuler™ DNA Ladder Mix (Thermo Scientific, MA, USA).

S3. Gel extraction and ligation into a cloning vector

Amplified PCR products were excised from the gel and the gel extraction procedure was performed using NucleoSpin® Gel and PCR Clean-up Kit (Macherey-Nagel, Düren, Germany). After gel extractions, eluents were run on 2.5% agarose gel and visualized.

Purified PCR fragments were ligated into pGEM®-T Easy T/A cloning vector (Promega). The composition of the ligation mixture is described in the article. The ligation reaction was incubated at 22°C for 1 h and to increase the ligation efficiency, they were also incubated at 4°C overnight. Before the transformation, T4 ligase was heat-inactivated at 70°C for 5 min.

S4. Transformation of chemically-competent Escherichia coli Top 10F′ cells

Cloning vectors carrying of *aphA*, *tetA* and 16S rRNA genes were used to transform chemically-competent *Escherichia coli* Top 10F′ cells. Cells transformed with pGEM®-T Easy vectors carrying PCR products were selected on Amp/X-gal/IPTG/LB plates. White colonies were restreaked on fresh Amp/X-gal/

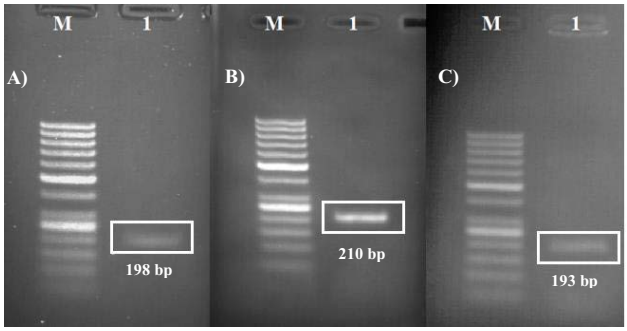

Fig. S2. PCR products in well 1 after amplification. (a) *aphA*, (b) *tetA*, and (c) 16S rRNA. Marker DNA: GeneRuler™ 50 bp DNA Ladder (Thermo Scientific, MA, USA).

Table S1
Gene-specific primer sequences, the corresponding PCR annealing temperatures, and amplicon sizes

Primer	Target	Sequence (5′–3′)	PCR annealing temperature (°C)	Amplicon size (bp)
*aphA*_FW	*aphA*	CGACGGGTAGAGCAAAGGT	62	198
*aphA*_RV		AGCGGACAGCATCAGTAA		
*tetA*_FW	*tetA*	GCTACATCCTGCTTGCCTTC	56	210
*tetA*_RV		CATAGATCGCCGTGAAGAGG		
16S_FW	16S rRNA	CCTACGGGAGGCAGCAG	58	193
16S_RV		ATTACCGCGGCTGCTGGG		

IPTG/LB plates. Colonies maintaining white color were screened to check the presence of inserts.

S5. Screening Escherichia coli Top 10F′ transformants with plasmid isolation and restriction digestion

White transformants were inoculated into 4 mL of LB-Amp broth and cultures were incubated at 37°C for 16 h at 200 rpm orbital shaking. 2 mL of cultures were used for plasmid isolation. After plasmid isolation, eluents were run on 1% (w/v) agarose gel at 120 V for 40 min. RedSafe™ Nucleic Acid Staining Solution (iNtRON) was used to visualize gels under UV transillumination. After that, plasmids were digested with the EcoRI restriction enzyme to release insert. Enzymatic digestion reactions were performed as recommended in the manufacturer's protocols (Thermo Scientific, MA, USA). The PCR products and cloning vectors were digested with a reaction mix containing 5U of the enzyme for each μg of DNA and 1X digestion buffer at 37°C for 1 to 5 h. Digested products were run on 1% agarose gels for visualization. Plasmid restriction for 16S-rRNA, *aphA*, and *tetA* screening were shown in Figs. S3–S5, respectively.

S6. Construction of the standard curve

Standard curves quantitative-polymerase chain reaction (Q-PCR) reaction was prepared following the instructions described in the main article. Ct values corresponding to copy numbers of 16S rRNA, *aphA* and *tetA* were plotted as in Figs. S6, S8, and S10, respectively. Also, thermal melting curves were constructed after the melting curve analysis following the quantification step is given in Figs. S7, S9, and S11. Q-PCR efficiency was above 80% and the R^2 value was >0.99 for the standard curve. Template concentrations were kept below 0.25 ng μL^{-1} to prevent product inhibition. The specificity of amplified fragments was confirmed by melting curves.

S7. Viable cell counts

100 mL of samples are used to measure viable cells. Bacterial cells within 100 mL of samples were collected with centrifugation at 10,000 xg for 30 min. After centrifugation, the cell pellet was re-suspended in 1 mL of sterile simulated urban wastewater. Thus, cell density in each sample was

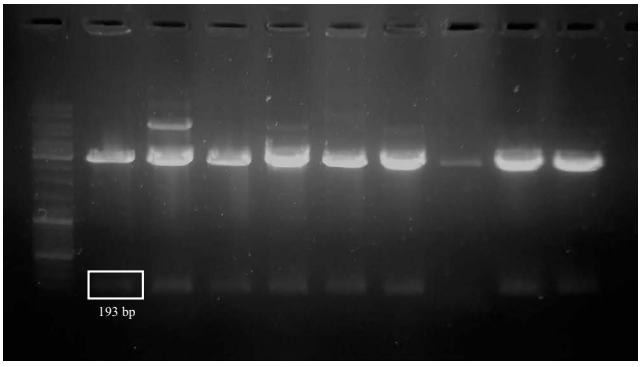

Fig. S3. EcoRI digestion 16S rRNA/pGEM-T plasmids. Marker DNA: GeneRuler™ DNA Ladder Mix (Thermo Scientific, MA, USA).

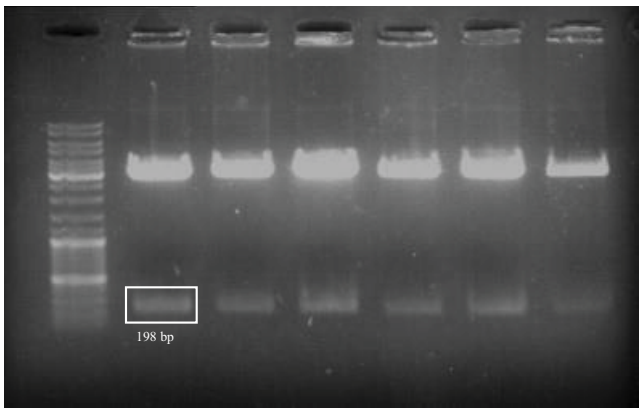

Fig. S4. EcoRI digestion *aphA*/pGEM-T plasmids. Marker DNA: GeneRuler™ DNA Ladder Mix (Thermo Scientific, MA, USA).

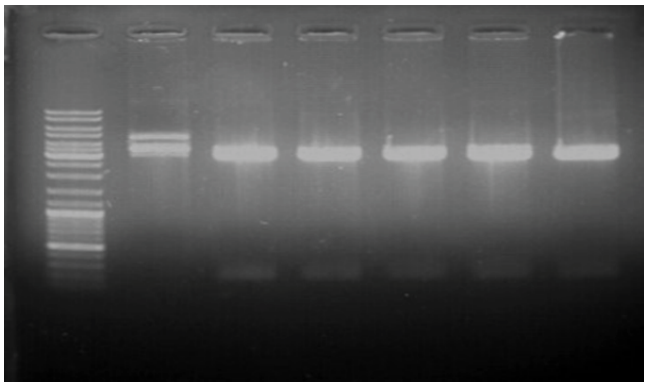

Fig. S5. EcoRI digestion *tetA*/pGEM-T plasmids. Marker DNA: GeneRuler™ DNA Ladder Mix (Thermo Scientific, MA, USA).

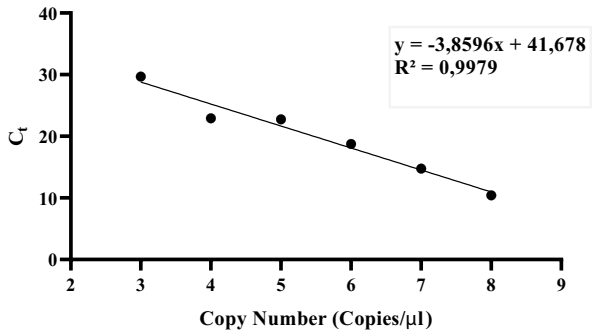

Fig. S6. Standard curve for the 16S rRNA gene used for copy number determination in Q-PCR.

100-fold concentrated to increase cell capture efficiency to prevent the recovery error. 10-fold dilution series were prepared up to 1:10^6 and 100 μL from each dilution was spread on the Luria-Bertani (LB) broth supplemented with Ampicillin (100 μg/mL), Kanamycin (50 μg/mL) and Tetracyclin (16 μg/mL) (AMP/KAN/TET/LB). Colonies after incubation were counted in plates having 30-300 colonies which are the statistically-reliable range. Colony-forming unit (CFU) describes a single viable cell that grows and reproduces and eventually forms a colony. CFU ml^{-1} is calculated using the formula given below, considering the 1:100-fold concentration before.

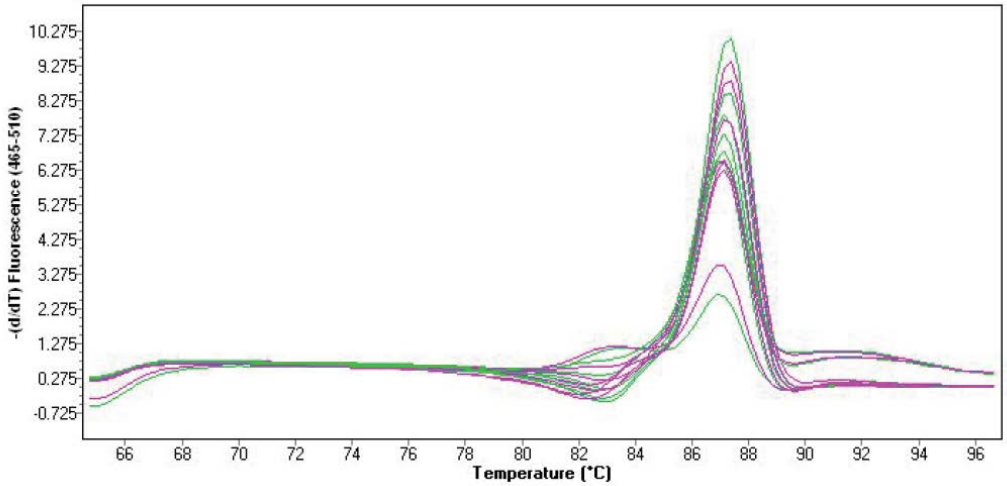

Fig. S7. The thermal melting curve belongs to the standard curve of the 16S rRNA gene.

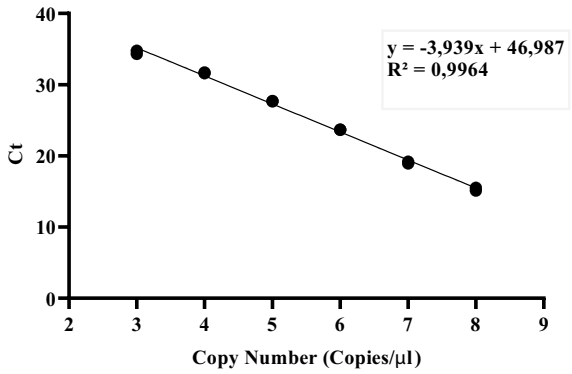

Fig. S8. Standard Curve for *aphA* gene used for copy number determination in Q-PCR.

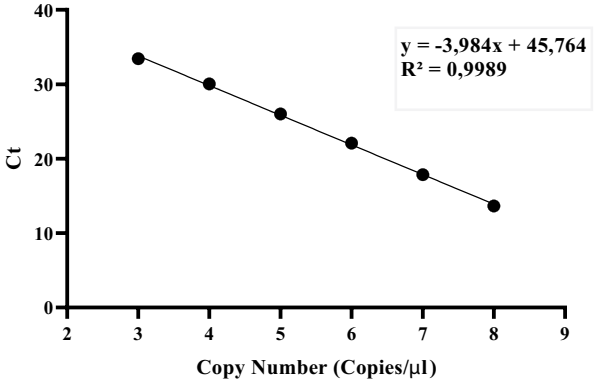

Fig. S10. Standard Curve for the *tetA* gene used for copy number determination in Q-PCR.

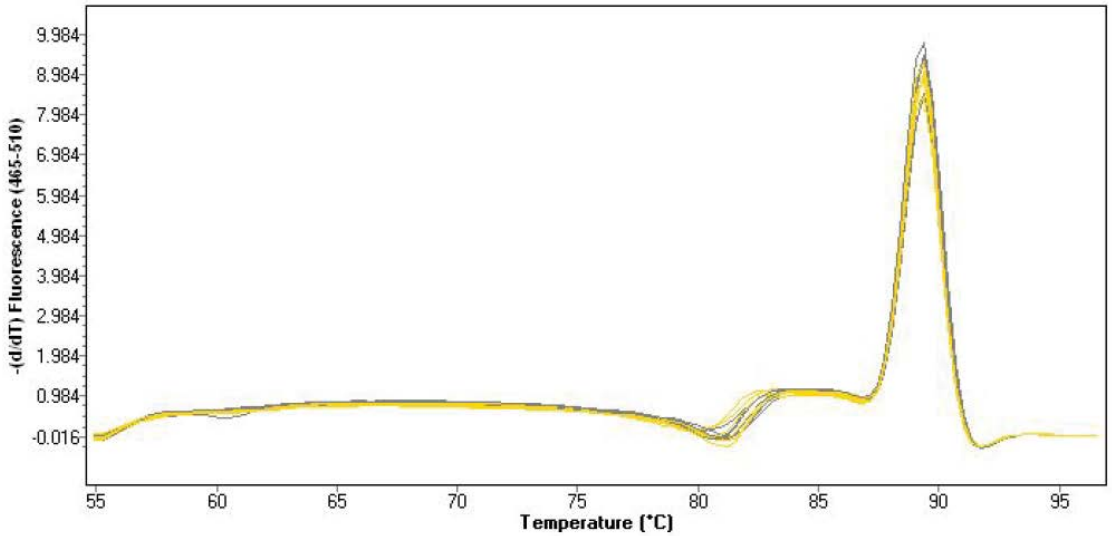

Fig. S9. The thermal melting curve belongs to the standard curve of *aphA* gene.

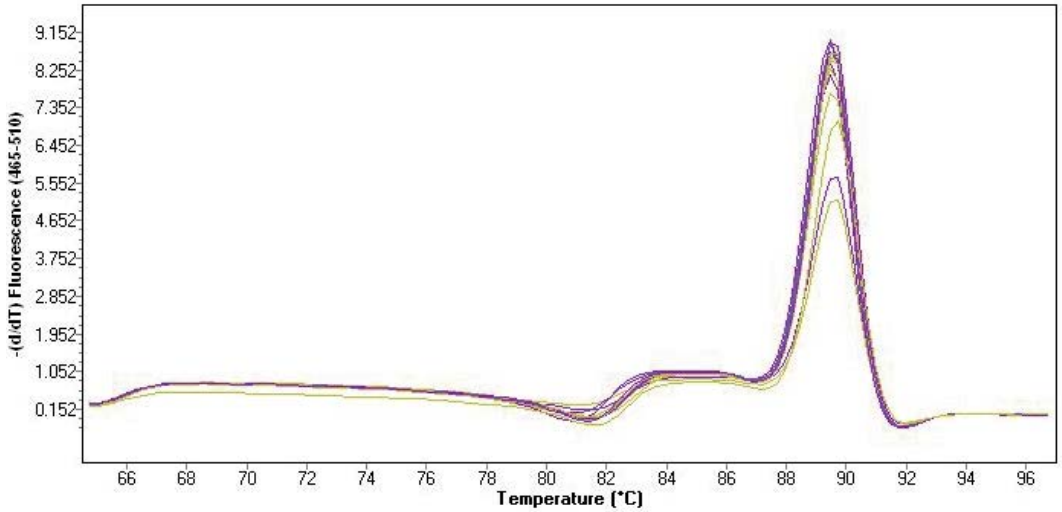

Fig. S11. The thermal melting curve belongs to the standard curve of the *tetA* gene.

$$\frac{\text{CFU}}{\text{ml}} = \frac{\left(\text{Number of colonies}\right)\times\left(\text{Dilution factor}\right)}{\text{Inoculation volume}\left(\text{ml}\right)} \times \frac{1}{100} \quad \text{(S1)}$$

After the number of colonies was determined before and after the treatment processes, log reduction (logR) values of each treatment process were calculated and given in Table S2. logR values were used to indicate the efficiency of an antimicrobial agent/treatment. According to this, 1, 2, and 3 log reduction correspond to 90%, 99%, and 99.9% reduction in viable cell number, respectively. logR is calculated using the formula given below, where 'N_o' is the viable cells number before treatment (at time = t_0) and 'N' is the viable cells number after treatment (at time = t).

$$\log R = \log \frac{N_o}{N} \quad \text{(S2)}$$

S8. Total DNA Isolation and Control PCRs of Samples

Total DNA isolations were conducted using the FastDNA® SPIN Kit (MP). Each filter paper was cut into small pieces using sterile scissors. These pieces were placed

Table S2
Viable cell counts and corresponding logR values

Treatment	CFU mL^{-1} (Mean)	Standard deviation	LogR	Standard deviation
UV-C (0 min)	1.04×10^6	0.14	–	–
UV-C (5 min)	1	0	6.01	0.06
UV-C (20 min)	1	0	6.01	0.06
O_3 (0 min)	3.32×10^5	0.88	–	–
O_3 (1 min)	2.27×10^5	0.09	0.15	0.10
O_3 (5 min)	5.5	1.5	4.78	0.004
HOCl (0 mg L^{-1})	3.2×10^5	1.1	–	–
HOCl (10 mg L^{-1})	1	0	5.48	0.16
HOCl (100 mg L^{-1})	1	0	5.48	0.16
Fe(0)HP/(FeOOH)HP (0 min)	1.28×10^6	0.26	–	–
Fe(0)/HP (20 min)	8.35×10^5	0.35	0.18	0.06
FeOOH/HP (60 min)	1.18×10^6	0.16	0.03	0.002
(Fe(II))HP/UV-A (0 min)	2.03×10^5	0.35	–	–
HP/UV-A (20 min)	7.35×10^2	0.35	3.44	0.05
Fe(II)/HP/UV-A (80 min)	3.16×10^1	0.7	4.82	0.04
(Fe(III))HP/UV-A (0 min)	4.34×10^6	0.39	–	–
Fe(III)/HP/UV-A (80 min)	6.1×10^2	0.7	3.85	0.01

inside the Lysing Matrix A tube. Then, 1 mL of cell lysis solution-TC buffer was added into the tube. After cells were homogenized for 40 s, Lysing Matrix A tubes were centrifuged at 14,000 xg for 10 min. 700–800 μL of supernatant was transferred to a 2.0 mL microcentrifuge tube. An equal volume of the Binding Matrix was added on top of supernatant and the tube was inverted to mix. The tube was gently agitated for 5 min at room temperature on a rotator. Then, half of the suspension was transferred to a SPIN™ Filter column. The SPIN™ Filter column was centrifuged at 14,000 xg for 1 min. The flow-through in the Catch Tube was discarded and the rest of the suspension was added to the column and centrifuged as indicated before. 500 μL of SEWS-M buffer was used to gently re-suspend the pellet in the column. The column was centrifuged at 14,000 xg for 1 min. The flow-through was discarded. The column was centrifuged at 14,000 xg for 2 min without adding any liquid. The Catch Tube was replaced with a clean tube. 100 μL of DNA elution solution was used to gently resuspend the Binding Matrix. The column was incubated at 55°C for 5 min in a heat block. Then, it was centrifuged at 14,000 xg for 1 min to collect the total DNA. Isolated total DNAs were visualized using agarose gel electrophoresis after treatment with UV-C radiation (Fig. S12), ozonation (Fig. S14), chlorination (Fig. S18) and homogenous photochemical iron-based AOPs (Fig. S20).

Before Q-PCR analysis, we employed standard PCR analysis (control PCR) to check whether any quantifiable genomic DNA represented by 16S rRNA and plasmid RP4 DNA represented by *aphA* and *tetA* are present in the isolated total DNA samples. For this, *aphA*, *tetA* and 16S rRNA genes were amplified by using isolated total DNA samples as template. DreamTaq Polymerase (Thermo Fischer Scientific) kit was used to set up PCR reactions. Primer sets used to amplify *aphA*, *tetA* and 16S rRNA genes and annealing temperatures of PCR reactions are given in Table S1. After amplification, PCR products were checked on 1% (w/v) agarose gel at 120 V for 40 min. After treatment with UV-C radiation (Fig. S13), ozonation (Figs. S15–S17), chlorination (Fig. S19), Fe(II)/HP/UV-A (Fig. S21) and Fe(III)/HP/UV-A (Fig. S22).

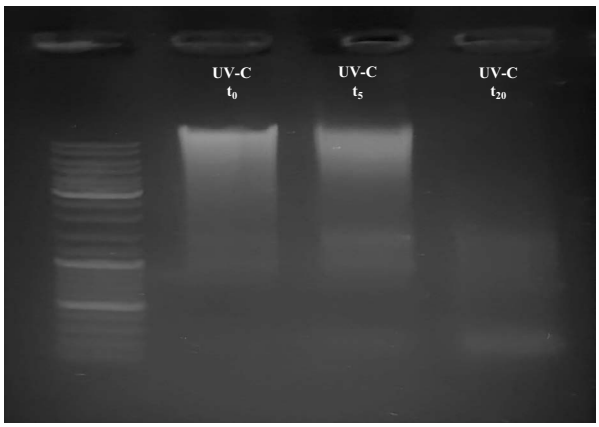

Fig. S12. Total DNA isolation from before (t_0) and after treatment with UV-C radiation for 5 min (t_5) and 20 min (t_{20}) samples. Marker: GeneRuler™ Ladder Mix (Thermo Scientific, MA, USA).

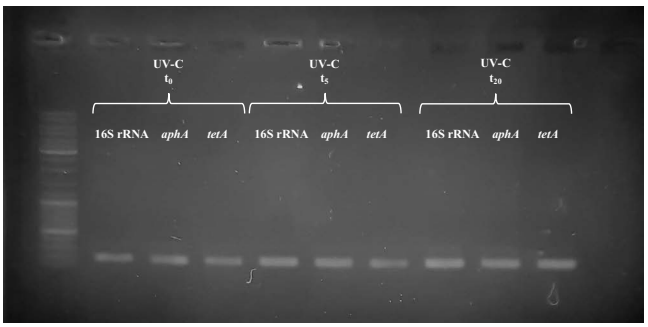

Fig. S13. Control PCR products of 16S rRNA, *aphA* and *tetA* before (t_0) and after treatment with UV-C radiation for 5 min (t_5) and 20 min (t_{20}) samples. Marker: GeneRuler™ Ladder Mix (Thermo Scientific, MA, USA).

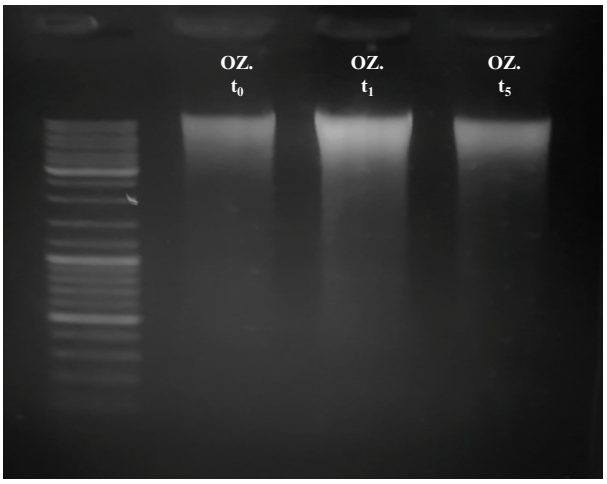

Fig. S14. Total DNA isolation from before (t_0) and after treatment with ozonation for 1 min (t_1) and 5 min (t_5). Marker: GeneRuler™ Ladder Mix (Thermo Scientific).

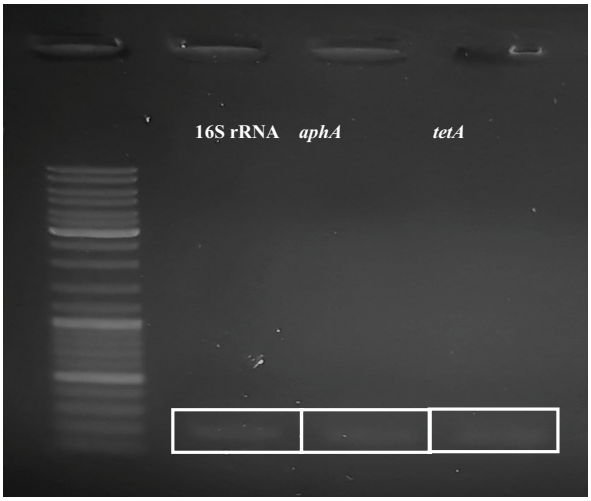

Fig. S15. Control PCR products of 16S rRNA, *aphA* and *tetA* of before (t_0) sample with ozonation. Marker: GeneRuler™ Ladder Mix (Thermo Scientific, MA, USA).

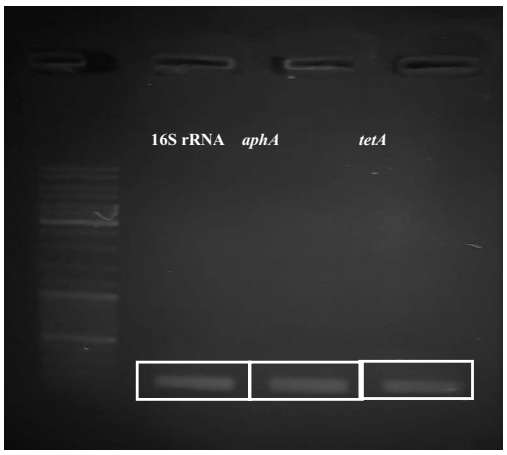

Fig. S16. Control PCR products of 16S rRNA, *aphA* and *tetA* of after 1 min-treatment (t_1) with ozonation. Marker: GeneRuler™ Ladder Mix (Thermo Scientific, MA, USA).

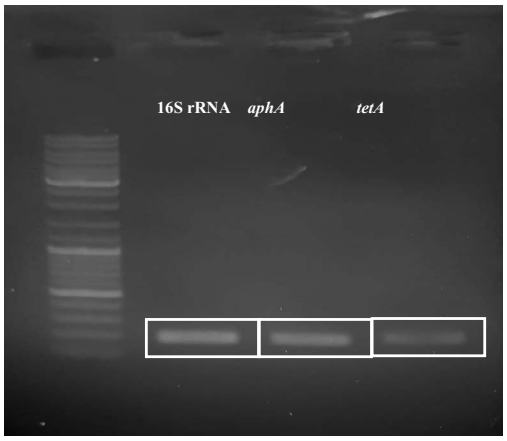

Fig. S17. Control PCR products of 16S rRNA, *aphA* and *tetA* of after 5 min-treatment (t_5) with ozonation. Marker: GeneRuler™ Ladder Mix (Thermo Scientific, MA, USA).

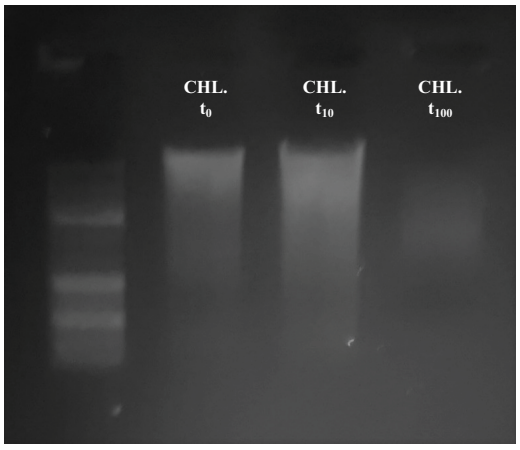

Fig. S18. Total DNA isolation from before (t_0) and after treatment samples with 10 mg mL^{-1} (t_{10}) and 100 mg mL^{-1} (t_{100}) chlorine. Marker: GeneRuler™ Ladder Mix (Thermo Scientific, MA, USA).

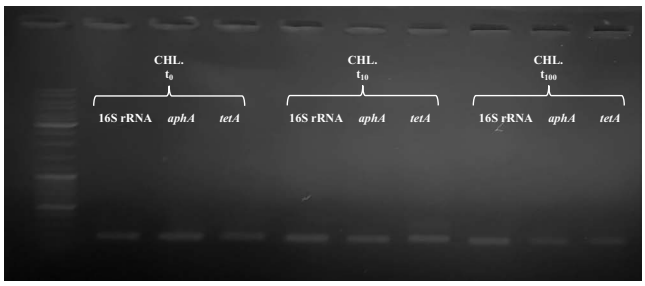

Fig. S19. Control PCR products of 16S rRNA, *aphA* and *tetA* before (t_0) and after treatment samples with 10 mg mL^{-1} (t_{10}) and 100 mg mL^{-1} (t_{100}) chlorine. Marker: GeneRuler™ Ladder (Thermo Scientific, MA, USA).

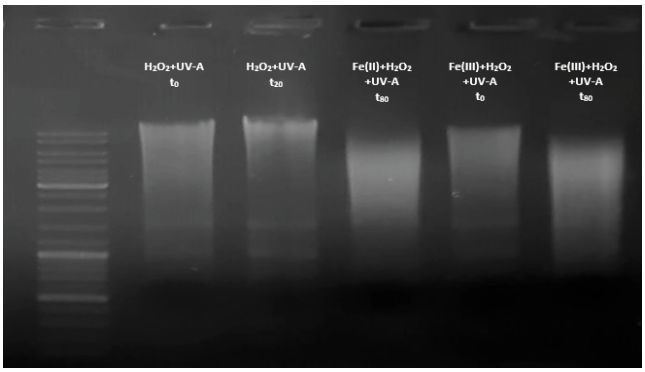

Fig. S20. Total DNA isolation from before and after iron-based homogenous photochemical treatment. Marker DNA: GeneRuler™ DNA Ladder mix (Thermo Scientific, MA, USA).

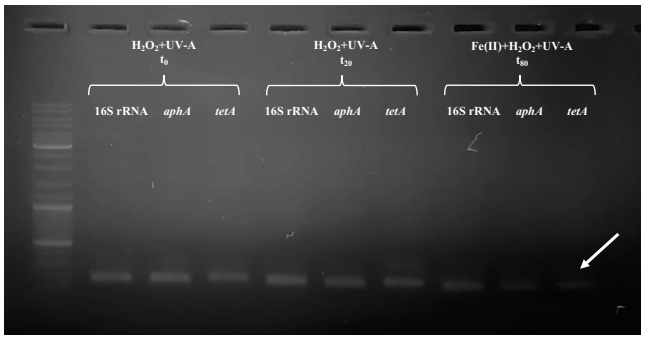

Fig. S21. Control PCR products of 16S rRNA, *aphA* and *tetA* before and after treatment with Fe(II)/HP/UV-A samples. Marker DNA: GeneRuler™ DNA ladder mix (Thermo Scientific, MA, USA).

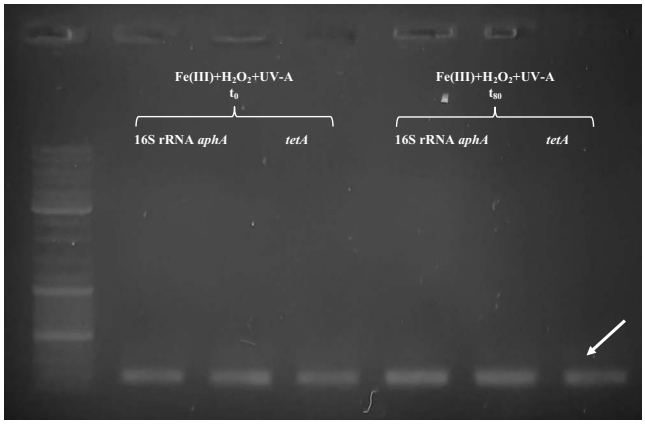

Fig. S22. Control PCR products of 16S rRNA, *aphA* and *tetA* before and after treatment with Fe(III)/HP/UV-A samples. Marker DNA: GeneRuler™ DNA ladder mix (Thermo Scientific, MA, USA).

S9. Determination gene copy numbers by Q-PCR

Copy numbers before and after treatment processes were determined according to the constructed standard curve. Ct values and copy numbers of 16S rRNA, *aphA* and *tetA* are shown in Table S3–S5, respectively. Copy number of 16S rRNA, *aphA* and *tetA* were calculated according to the formula given below where 'Ct' is threshold cycle number obtained by Q-PCR, *a* and *b* are constants obtained by standard curves ($y = ax + b$), 'Df' corresponds to the dilution rate of total DNA sample used as template for Q-PCR reactions, and '*V*' corresponds to the volume of sample used for total DNA isolation before or after treatment.

$$\frac{\text{Copies}}{\text{mL}} = \frac{10^{\frac{\text{Ct}-b}{a}} \times \text{Df}}{V} \tag{S3}$$

Then, log reduction values of gene copy numbers were calculated similarly to log reduction in viable cell counts in Section 7. In this case, 'Co' represents the gene copy number before treatment (to) while '*C*' represents the gene copy number after-treatment processes.

Table S3
Ct values of before and after treatments obtained by Q-PCR and log(reduction) values of 16S rRNA. Obtained Ct values were used to calculate copy numbers of 16S rRNA according to the formula of both standard curve and the dilution factors of template prepared from total DNA extracts

Treatment	Q-PCR Ct values		Copy number (Mean)	Standard deviation	Log *R* (Mean)	Standard deviation
UV-C (0 min) (to)	23.21	23.06	1.28×10^8	0.06	–	–
UV-C (5 min)	31.89	32.03	2.64×10^5	0.11	2.68	0.04
UV-C (20 min)	32.5	32.75	1.78×10^5	0.13	2.86	0.05
O_3 (0 min) (to)	24.77	24.82	4.74×10^7	0.07	–	–
O_3 (1 min)	22.79	22.74	4.54×10^7	0.06	0.02	0.01
O_3 (5 min)	23.89	23.81	2.38×10^7	0.05	0.30	0.02
HOCl (0 mg L^{-1}) (to)	24	24.29	7.00×10^7	0.60		
HOCl (10 mg L^{-1})	23.35	23.57	3.51×10^7	0.23	0.30	0.01
HOCl (100 mg L^{-1})	28.98	29.53	1.34×10^6	0.22	1.72	0.03
(Fe(II))HP/UV-A (0 min) (to)	23.97	23.54	8.88×10^7	1.13	–	–
HP/UV-A (20 min)	22.76	24.91	3.39×10^7	1.92	0.50	0.22
Fe(II)/HP/UV-A (80 min)	23.42	23.01	4.08×10^7	0.50	0.34	0.00
(Fe(III))HP/UV-A (0 min) (to)	23.25	23.31	1.17×10^8	0.02	–	–
Fe(III)/HP/UV-A (80 min)	22.92	23.11	4.57×10^7	0.26	0.41	0.02

Table S4
Ct values of before and after treatments obtained by Q-PCR and log(reduction) values of *aphA*. Obtained Ct values were used to calculate copy numbers of *aphA* according to the formula of both standard curve and the dilution factors of template prepared from total DNA extracts

Treatment	Q-PCR Ct values		Copy Number (Mean)	Standard deviation	Log *R* (Mean)	Standard deviation
UV-C (0 min) (to)	23.21	23.06	1.38×10^8	0.11	–	–
UV-C (5 min)	31.89	32.03	3.80×10^5	0.33	2.56	0.07
UV-C (20 min)	32.5	32.75	4.75×10^4	0	3.50	0.00
O_3 (0 min) (to)	24.77	24.82	3.41×10^7	0.51	–	–
O_3 (1 min)	22.79	22.74	2.50×10^7	0.20	0.13	0.10
O_3 (5 min)	23.89	23.81	1.90×10^7	0.13	0.25	0.10
HOCl (0 mg L^{-1}) (to)	24	24.29	4.08×10^7	0.27	–	–
HOCl (10 mg L^{-1})	23.35	23.57	1.38×10^7	0,87	0.58	0.29
HOCl (100 mg L^{-1})	28.98	29.53	6.31×10^5	1,64	1.82	0.09
(Fe(II))HP/UV-A (0 min) (to)	23.97	23.54	2.53×10^7	0,41	–	–
HP/UV-A (20 min)	22.76	24.91	1.53×10^7	0.63	0.25	0.12
Fe(II)/HP/UV-A (80 min)	23.42	23.01	7.92×10^6	0.97	0.50	0.02
(Fe(III))HP/UV-A (0 min) (to)	23.25	23.31	6.14×10^7	3.96	–	–
Fe(III)/HP/UV-A (80 min)	22.92	23.11	1.45×10^7	0.32	0.52	0.24

Table S5
Ct values of before and after treatments obtained by Q-PCR and log(Reduction) values of *tetA*. Obtained Ct values were used to calculate copy numbers of *tetA* according to the formula of both standard curve and the dilution factors of template prepared from total DNA extracts

Treatment	Q-PCR Ct values		Copy number (Mean)	Standard deviation	Log *R* (Mean)	Standard deviation
UV-C (0 min) (to)	27.55	27.08	8.63×10^7	1,16	–	–
UV-C (5 min)	32.69	33.02	1.40×10^6	0.13	1.79	0.10
UV-C (20 min)	37.36	35.5	2.02×10^5	0.99	2.69	0.17
O_3 (0 min) (to)	28.94	29.32	3.01×10^7	0.33		
O_3 (1 min)	26.82	26.79	3.28×10^7	0.03	–0.04	0.05
O_3 (5 min)	27.5	27.3	2.33×10^7	0.13	0.11	0.07
HOCl (0 mg L^{-1}) (to)	28.29	28.14	5.09×10^7	0.22	–	–
HOCl (10 mg L^{-1})	27.69	27.43	2.48×10^7	0.19	0.31	0.01
HOCl (100 mg L^{-1})	32.97	36.63	7.29×10^5	5,72	2.05	0.48
(Fe(II))HP/UV-A (0 min) (to)	27.7	28.11	6.12×10^7	0.72	–	–
0HP/UV-A (20 min)	26.92	27.35	3.19×10^7	0.39	0.28	0.00
Fe(II)/HP/UV-A (80 min)	28.11	27.04	2.57×10^7	0.77	0.39	0.19
(Fe(III))HP/UV-A (0 min) (to)	28.55	27.09	6.96×10^7	2.77	–	–
Fe(III)/HP/UV-A (80 min)	28.04	28.41	1.69×10^7	0.18	0.58	0.23